MOLECULAR AND CELLULAR BIOLOGY, Oct. 1999, p. 7123–7137 Vol. 19, No. 10
0270-7306/99/$04.00+0

Hsl7 Localizes to a Septin Ring and Serves as an Adapter in a Regulatory Pathway That Relieves Tyrosine Phosphorylation of Cdc28 Protein Kinase in *Saccharomyces cerevisiae*

MARK J. SHULEWITZ, CARLA J. INOUYE,† AND JEREMY THORNER*

Department of Molecular and Cell Biology, Division of Biochemistry and Molecular Biology, University of California, Berkeley, California 94720-3202

Received 25 March 1999/Returned for modification 13 May 1999/Accepted 22 June 1999

Successful mitosis requires faithful DNA replication, spindle assembly, chromosome segregation, and cell division. In the budding yeast *Saccharomyces cerevisiae*, the G_2-to-M transition requires activation of Clb-bound forms of the protein kinase, Cdc28. These complexes are held in an inactive state via phosphorylation of Tyr19 in the ATP-binding loop of Cdc28 by the Swe1 protein kinase. The *HSL1* and *HSL7* gene products act as negative regulators of Swe1. Hsl1 is a large (1,518-residue) protein kinase with an N-terminal catalytic domain and a very long C-terminal extension. Hsl1 localizes to the incipient site of cytokinesis in the bud neck in a septin-dependent manner; however, the function of Hsl7 was not previously known. Using both indirect immunofluorescence with anti-Hsl7 antibodies and a fusion of Hsl7 to green fluorescent protein, we found that Hsl7 also localizes to the bud neck, congruent with the septin ring that faces the daughter cell. Both Swe1 and a segment of the C terminus of Hsl1 (which has no sequence counterpart in two Hsl1-related protein kinases, Gin4 and Kcc4) were identified as gene products that interact with Hsl7 in a two-hybrid screen of a random *S. cerevisiae* cDNA library. Hsl7 plus Swe1 and Hsl7 plus Hsl1 can be coimmunoprecipitated from extracts of cells overexpressing these proteins, confirming that Hsl7 physically associates with both partners. Also consistent with the two-hybrid results, Hsl7 coimmunoprecipitates with full-length Hsl1 less efficiently than with a C-terminal fragment of Hsl1. Moreover, Hsl7 does not localize to the bud neck in an *hsl1*Δ mutant, whereas Hsl1 is localized normally in an *hsl7*Δ mutant. Phosphorylation and ubiquitinylation of Swe1, preludes to its destruction, are severely reduced in cells lacking either Hsl1 or Hsl7 (or both), as judged by an electrophoretic mobility shift assay. Collectively, these data suggest that formation of the septin rings provides sites for docking Hsl1, exposing its C terminus and thereby permitting recruitment of Hsl7. Hsl7, in turn, presents its cargo of bound Swe1, allowing phosphorylation by Hsl1. Thus, Hsl1 and Hsl7 promote proper timing of cell cycle progression by coupling septin ring assembly to alleviation of Swe1-dependent inhibition of Cdc28. Furthermore, like septins and Hsl1, homologs of Hsl7 are found in fission yeast, flies, worms, and humans, suggesting that its function in this control mechanism may be conserved in all eukaryotes.

Correct progression of the events of the eukaryotic cell cycle is essential for successful division. Cellular components, especially chromosomes, must be accurately replicated and faithfully segregated between the mother and daughter cells. To accomplish this partitioning with high fidelity, mechanisms have evolved to monitor the proper execution of these processes and to impose a delay in cell cycle progression to allow for repair of any damage or mistakes that may have occurred. These control mechanisms have been termed checkpoints (38). Checkpoints triggered by DNA damage (90), by errors in DNA replication (89), and by defects in spindle assembly and kinetochore attachment (33, 85) have been uncovered by genetic analysis in budding and fission yeasts (for reviews, see references 36 and 65). A checkpoint that delays cytokinesis in response to spindle misalignment also has been described (61). Additional control mechanisms must exist to impose the intricate choreography of cell cycle events.

In particular, some feedback control must assess the status of the incipient daughter and impose a delay until the recipient cell is big enough to accept its complement of chromosomes before the cell commits to mitosis. Indeed, in *Saccharomyces cerevisiae*, such a morphology checkpoint may be based on mechanisms that monitor the state of assembly of the actin cytoskeleton because cells exhibit a delay in G_2 when the actin cytoskeleton is perturbed (53, 56). Even if a daughter is of sufficient size, a cell also needs a mechanism that gauges the state of assembly of the cytokinesis apparatus and imposes a delay until the cleavage machinery is properly assembled and ready to operate before allowing chromosomes to be segregated by the mitotic spindle. Indeed, there seems to be a cytokinesis checkpoint in yeast that monitors formation of a distinct cytoskeletal structure, the septin rings (which mark the incipient site of cell division), because defects in septin assembly also cause a G_2 delay (5). Imposition of both of these checkpoints requires the function of the Swe1 protein kinase (5, 79), a homolog of *Schizosaccharomyces pombe* Wee1 (74). Swe1 is a negative regulator of the Cdc28 protein kinase (6).

Major stages of the *S. cerevisiae* cell cycle are initiated by action of the *CDC28* gene product (reviewed in reference 57), a founding member of the conserved family of cyclin-dependent kinases (CDKs) (reviewed in reference 59). Cdc28 associates with different sets of cyclins to mediate different cell cycle transitions. Mitotic events are controlled by Cdc28 bound to a set of functionally redundant B-type cyclins, Clb1, Clb2, Clb3, and Clb4 (26, 62). Clb-bound Cdc28 is susceptible to

* Corresponding author. Mailing address: Department of Molecular and Cell Biology, Room 401, Barker Hall, Corner of Hearst and Oxford St., Berkeley, CA 94720-3202. Phone: (510) 642-2558. Fax: (510) 643-5035. E-mail: jeremy@socrates.berkeley.edu.

† Present address: Tjian Laboratory, Howard Hughes Medical Institute, University of California, Berkeley, CA 94720-3204.

inhibitory phosphorylation on a conserved residue (Tyr19) in its ATP-binding loop mediated by Swe1, and phosphorylation of Cdc28-Clb complexes on Tyr19 blocks entry into mitosis (6). The regulatory role of phosphorylation at Tyr19 in Cdc28 was not appreciated until recently because a Y19F mutation does not have catastrophic consequences (2, 82), unlike the equivalent mutation in the corresponding fission yeast CDK (Cdc2) (31). Phosphorylation at Tyr19 can be reversed by the phosphoprotein phosphatase Mih1 (72), a homolog of *S. pombe* Cdc25 (73). Thus, a potential cause of the delay in entry into mitosis provoked by the septin-based cytokinesis checkpoint is blockade of Cdc28 activity via phosphorylation at Tyr19 due to activation of Swe1 or inhibition of Mih1 (or both). Conversely, in a normal cell cycle, proper septin assembly must trigger events that assist in preventing phosphorylation of Cdc28 at Tyr19.

The septins are a family of proteins, originally identified in budding yeast (35, 54) but conserved in all eukaryotes (16). Loss-of-function septin mutations cause cytokinesis defects in yeast (8, 37), in *Drosophila melanogaster* (63), and in mice (48). In *S. cerevisiae*, septins involved in mitotic cell division are encoded by the *CDC3*, *CDC10*, *CDC11*, and *CDC12* genes, assemble into 10-nm filaments (9), and colocalize at the bud neck (54). In vitro, these septins form a tight complex and can assemble into long filaments (27). As visualized by indirect immunofluorescence, the septins appear to form two stacked rings. The apparent plane of the rings is orthogonal to the mother-bud axis; one ring faces the mother cell, and the other faces the daughter. However, there is evidence that the rings may instead represent the prominent lips of a continuous cylindrical collar formed by lateral association of septin filaments parallel to the mother-bud axis (25a, 54a). Under restrictive conditions, temperative-sensitive septin mutants exhibit elongated buds and display biochemical hallmarks of cells delayed in cell cycle progression (11, 17). The precise contribution of septins to cell division is not entirely understood, but it has been suggested that septins form a landmark or scaffold necessary for the recruitment and/or spatial organization of other structures (e.g., actomyosin) required for cytokinesis (19).

How the state of septin assembly transduces a signal that modulates Tyr19 phosphorylation in Cdc28 is not well understood. Clues about the mechanism have come, first, from the demonstration that Hsl1, a protein kinase that is a homolog of *S. pombe* Nim1 (75), and Hsl7, a protein of previously unknown function, are negative regulators of Swe1 (55). Second, it has been shown recently that Hsl1 localizes to the septin ring and can physically associate with at least one septin (5). Moreover, autophosphorylation of Hsl1 requires an intact septin ring (5), suggesting that assembled septin structures stimulate the catalytic activity of Hsl1. Thus, the state of septin assembly may regulate Swe1 via Hsl1. However, the role of Hsl7 in this regulatory mechanism has been obscure. The primary structure of Hsl7, unlike that of Hsl1, does not possess sequence features diagnostic of any protein of known function. Nonetheless, readily recognizable homologs of Hsl7 are present in all eukaryotes that can be readily examined, including fission yeast (30), *Caenorhabditis elegans* (55), and humans (49). Skb1, the *S. pombe* Hsl7 homolog, reportedly interacts with members of the PAK (p21-activated protein kinase) family, as judged by the yeast two-hybrid assay (30), which raised the possibility that Hsl7 itself can serve as a linker or scaffold to assembly or localize a signaling complex. To address its function, we developed reagents to examine the subcellular distribution of Hsl7 and to determine the nature of the other proteins with which Hsl7 interacts. Here we describe our findings, which provide considerable insight as to how Hsl7 participates in the septin assembly checkpoint and assists in communicating a signal from Hsl1 to Swe1.

MATERIALS AND METHODS

Strains and growth conditions. Yeast strains used in this study are listed in Table 1. Two *hsl7* null alleles were constructed. The *hsl7-Δ10* mutation was generated by using PCR to amplify the 3′ end of the *HSL7* gene and its immediately flanking DNA, using appropriate primers and genomic DNA of strain W303 as the template. The resulting product (with *Eco*RI ends) was ligated into *Eco*RI-digested pUC19 (93) carrying a 3.8-kb *Bam*HI-*Bgl*II fragment containing an *hisG::URA3::hisG* cassette (1), yielding pCJ61. PCR was used to amplify the 5′ end of the *HSL7* gene and its immediately flanking DNA, and the resulting product (with flush ends) was ligated with *Xba*I-digested pCJ61 that had been converted to blunt ends by incubation with T4 DNA polymerase, yielding pCJ65. A 6.3-kb *Msc*I-*Sal*I fragment of pCJ65 carrying the resulting *hsl7-Δ10*(*::hisG::URA3::hisG*) construct (in which codons 99 to 806 of *HSL7* have been deleted) was used for DNA-mediated transformation of the desired *ura3* yeast strains, selecting for Ura$^+$ colonies. To generate the *hsl7-Δ20* mutation, an internal 2-kb segment of the *HSL7* sequence (codons 83 to 740) was deleted from the Litmus-28-derived plasmid pMJS1 (see below) by complete digestion with *Xba*I and partial digestion with *Eco*RV and replaced with an *Xba*I-*Sma*I fragment carrying the *HIS3* gene, excised from pJJ215 (44), simultaneously eliminating the *Eco*RV site in the *HSL7* DNA, and yielding pMJS11. A 3.6-kb fragment carrying the resulting *hsl7-Δ20(::HIS3)* construct (in which *HIS3* is inserted in the same transcriptional orientation as *HSL7*) was excised from the polylinker in pMJS11 by digestion with *Stu*I and *Eco*RV and used for DNA-mediated transformation of the desired *his3* yeast strains, selecting for His$^+$ colonies. Correct transplacement of the *HSL7* locus on chromosome II was confirmed both by Southern hybridization analysis (83) and by PCR using appropriate primers and genomic DNA isolated from the transformants and the parental strain as templates. Standard rich (YP) and defined minimal (SC) media (78), containing either 2% glucose (Glc), 2% raffinose (Raf), or 2% galactose (Gal) as the carbon source and supplemented with the appropriate nutrients to maintain selection for plasmids, were used to culture yeast cells. For the two-hybrid screen, SCGlc-Leu-Trp-Ura plates were supplemented with 0.1 M potassium phosphate (pH 7.0) and 40 μg of 5-bromo-4-chloro-3-indolyl-β-D-galactopyranoside (X-Gal; American Biorganics, Inc.) per ml.

Plasmids and recombinant DNA methods. Plasmids were constructed by using standard procedures (76) in *Escherichia coli* DH5α (32), SURE (Stratagene, Inc.), or JM110 (93). Unless indicated otherwise, *Pfu*I DNA polymerase (Stratagene) was used for all PCRs. The lack of errors in constructs prepared by PCR was verified by nucleotide sequence analysis using the dideoxynucleotide chain termination method (77). To isolate genomic DNA carrying the *HSL7* gene, PCR was used to amplify the corresponding open reading frame from chromosome II (25) by using appropriate primers and genomic DNA of strain W303. The resulting fragment was radiolabeled by the random primer method (24) and used to screen a yeast genomic DNA library in the vector, pSB32 (gift of F. Spencer and P. Hieter, then at Johns Hopkins University School of Medicine, Baltimore, Md.). A 3.7-kb *Hin*dIII-*Hin*dIII fragment of genomic DNA carrying the entire *HSL7* locus and its flanking regions was excised from one of the plasmids isolated and inserted into the polylinker of *Hin*dIII-digested vector, Litmus-28 (23), yielding pMJS1.

To construct a fusion of full-length Hsl7 to glutathione *S*-transferase (GST), PCR with appropriate primers was used to introduce a *Bam*HI site upstream and immediately adjacent to the initiator codon of the *HSL7* coding sequence, yielding a derivative with the sequence 5′-GGA TCC **ATG** CAT AGC (*Bam*HI site underlined and Met codon in bold). For expression of the GST-Hsl7 chimera in *E. coli*, a *Bam*HI-*Eco*RI fragment containing the modified version of *HSL7* was inserted in frame into *Bam*HI- and *Eco*RI-digested pGEX-4T-1 (Pharmacia), yielding pGEX-HSL7. To produce a plasmid for expression of the GST-Hsl7 chimera in yeast, a 0.7-kb *Eco*RI-*Bam*HI fragment containing the bidirectional *GAL1/10* promoter (41) was excised from plasmid pMTL4 (gift of Stephen Johnston, University of Texas Southwestern Medical Center, Dallas) and inserted into the corresponding sites of the *LEU2*-marked vector, YEplac181 (28), yielding YEpLG. Next, PCR with appropriate primers and pGEX-KG (58) as the template was used to introduce a *Bgl*II site upstream of the initiator codon of the GST coding sequence, yielding a derivative with the sequence 5′-GGG AGA TCT ACA **ATG** TCC CCT-3′ (*Bgl*II site underlined and Met codon in bold). The resulting product was cleaved with *Bgl*II and *Msc*I and ligated, along with a 0.5-kb *Msc*I-*Hin*dIII fragment excised from pGEX-KG, into *Bam*HI- and *Hin*dIII-digested YEpLG, yielding YEpLG-GST. Finally, a 2.5-kb *Bam*HI-*Sal*I fragment excised from pGEX-HSL7 was inserted into the corresponding sites of YEpLG-GST, yielding YEpLG-GST-Hsl7.

To construct an in-frame fusion of *HSL7* to the Gal4 DNA-binding domain [Gal4(DBD)], PCR with appropriate primers was used to introduce a *Bam*HI site downstream of the termination codon of the *HSL7* coding sequence, yielding a derivative with the sequence 5′-**TGA** ATT CTG CAT TGG ATC C-3′ (stop codon in bold and *Bam*HI site underlined). An *Nde*I-*Bam*HI fragment containing this modified version of *HSL7* was ligated into an *Nde*I- and *Bam*HI-digested, 2μm DNA-based, *TRP1*-marked vector, pAS1 (21), yielding pAS1-HSL7, in which the Gal4(DBD)-Hsl7 fusion is expressed from the constitutive *ADH1*

TABLE 1. *S. cerevisiae* strains used

Strain	Genotype	Reference or source
W303	*MAT***a**/*MAT*α *ade2-1/ade2-1 can1-100/can1-100 his3-11,15/his3-11,15 leu2-3,112/leu2-3,112 trp1-1/trp1-1 ura3-1/ura3-1*	88
BYB67[a]	W303 *ADE2/ade2-1 LYS2/lys2*Δ*::hisG*	This study
YCJ677	BYB67 *hsl7-*Δ*10*(*hisG::URA3::hisG*)*/HSL7*	This study
MJY100[b]	*MAT***a** *ADE2 can1-100 his3-11,15 leu2-3,112 LYS2 trp1-1 ura3-1*	This study
MJY101[b]	*MAT*α *ade2-1 can1-100 his3-11,15 leu2-3,112 lys2*Δ*::hisG trp1-1 ura3-1*	This study
MJY102	MJY100 *hsl7-*Δ*20(::HIS3)*	This study
MJY107	MJY101 × MJY102	This study
MJY110[c]	*MAT*α *ADE2 can1-100 his3-11,15 leu2-3,112 lys2*Δ*::hisG trp1-1 ura3-1 hsl7-*Δ*20*	This study
MJY112[c]	*MAT***a** *ADE2 can1-100 his3-11,15 leu2-3,112 LYS2 trp1-1 ura3-1 HLS7*	This study
MAY1[d]	*MAT***a** *ade2-1 can1-100 his3-11,15 leu2-3,112 ura3-1 hsl1-*Δ*1(::URA3)*	55
MJY141[e]	*MAT***a** *ADE2 can1-100 his3-11,15 leu2-3,112 trp1-1 ura3-1 hsl1-*Δ*1 HSL7*	This study
MJY146[e]	*MAT*α *ADE2 can1-100 his3-11,15 leu2-3,112 trp1-1 ura3-1 hsl1-*Δ*1 hsl7-*Δ*20*	This study
SCY33	*MAT***a** *CDC28(Y19F)-HA::LEU2 his3 leu2 trp1 ura3*	B. Booher
MJY124[f]	*MAT***a** *his3 leu2 lys2::hisG trp1 ura3 hsl7-*Δ*20 CDC28(Y19F)-HA::LEU2*	This study
TDY22[g]	*MAT***a** *ade2 his6 leu2-3,112 lys2-333 trp1-289 ura3-52 sst1-3*	This study
MJY155[h]	*MAT***a** *HSL1 HSL7 his3 his6 leu2 lys2 trp1 ura3 sst1-3*	This study
MJY156[h]	*MAT***a** *HSL1 hsl7-*Δ*20 his3 his6 leu2 lys2 trp1 ura3 sst1-3*	This study
MJY157[h]	*MAT***a** *hsl1-*Δ*1 HSL7 his3 his6 leu2 lys2 trp1 ura3 sst1-3*	This study
MJY158[h]	*MAT***a** *hsl1-*Δ*1 hsl7-*Δ*20 his3 his6 leu2 lys2 trp1 ura3 sst1-3*	This study
YD116	*MAT***a** *ade2-101*^{oc} *can1 gal4-542 gal80-538 his3-*Δ*200 leu2-3,112 lys2-801*^{am} *trp1-901 ura3-52 ADE2::GAL1-URA3 LYS2::*UAS_{GAL}*-lacZ*	T. Durfee
BJ2168	*MAT***a** *leu2 trp1 ura3-52 prb1-1122 pep4-3 prc1-407 gal2*	42
Y190	*MAT***a** *ade2-101*^{oc} *cyh2 gal4 gal80 his3 leu2-3,112 trp1-901 ura3-52 URA3::GAL1-lacZ LYS2::*UAS_{GAL}*-HIS3*	3

[a] Derived from W303 by transformation, sequentially, with *ADE2*$^{+}$ DNA and a *lys2*Δ*::hisG::URA3::hisG* construct, followed by selection for a Ura^{-} segregant on 5-fluoro-orotic acid medium.
[b] Derived by tetrad dissection of BYB67.
[c] Derived by tetrad dissection of MJY107.
[d] Derived from W303.
[e] Segregant from a diploid (MJY110 × MAY1).
[f] Segregant from a diploid (MJY110 × SCY33).
[g] Segregant of diploid TDY21 (18).
[h] Segregant from a diploid (MJY146 × TDY22).

promoter. To construct *URA3*- and *LEU2*-marked vectors expressing *HSL7* from the *GAL1* promoter, a 2.8-kb fragment containing the *HSL7* coding sequence was excised from pGEX-HSL7 by cleavage with *Bam*HI and *Eco*RI and ligated into *Bam*HI- and *Eco*RI-digested vectors, YCpUG and YCpLG (4), yielding YCpUG-HSL7 and YCpLG-HSL7, respectively.

To tag the *HSL7* gene product with a c-Myc epitope recognized by the monoclonal antibody (MAb) 9E10 (22), PCR with appropriate primers was used to introduce a *Stu*I site very near the 3′ end, yielding a derivative with the sequence 5′-TCC AGG CCT CTG **TGA** ATT-3′ (*Stu*I site underlined and stop codon in bold). A *Spe*I-*Eco*RI fragment containing the 3′ portion of this modified version of *HSL7* was ligated with a 2.7-kb *Bam*HI-*Spe*I fragment containing the 5′ portion of *HSL7*, excised from pGEX-HSL7 into *Bam*HI- and *Eco*RI-digested vector, pGEM-7Zf(+) (Promega), yielding pGEM7Z-HSL7. An 81-bp blunt-ended double-stranded oligonucleotide encoding a c-Myc epitope (IEEQKLISEEDLLRKRD) was inserted in frame into the *Stu*I site in pGEM7Z-HSL7, yielding pGEM7Z-HSL7-Myc. Finally, for expression in yeast, a *Bam*HI-*Eco*RI fragment from pGEM7Z-HSL7-Myc was inserted into YCpUG, yielding YCpUG-Hsl7-Myc.

To construct an in-frame green fluorescent protein (GFP)-Hsl7 fusion, PCR was used with appropriate primers to create a derivative of GFP(F64L S65T) (gift of J. Waddle, Washington University, St. Louis, Mo.) flanked by *Nsi*I sites. The resulting modified GFP(F64L S65T) contains at its 5′ end the sequence, 5′-**ATG** CAT AAA GGA-3′ (*Nsi*I site underlined and start codon in bold) and at its 3′ end the sequence 5′-GAA CTA ATG CAT-3′. This cassette was excised by digestion with *Nsi*I and inserted into the corresponding site in YCpLG-HSL7, yielding YCpLG-GFP-HSL7, and correct orientation was confirmed by appropriate restriction endonuclease digestion. To express the same fusion from the *HSL7* promoter on a low-copy-number (*CEN*) plasmid, first, the *HSL7* promoter was excised from pMJS1 by digestion with *Nde*I followed by digestion with *Nsi*I, and the resulting 0.45-kb *Nsi*I-*Nde*I fragment was ligated along with a 2.5-kb *Nde*I-*Hin*dIII fragment containing the entire *HSL7* open reading frame into *Pst*I- and *Hin*dIII-digested vector, YCplac22 (28), yielding YCpT-HSL7. The 0.8-kb *Nsi*I-*Nsi*I fragment containing the GFP(F64L S65T) cassette was then inserted into the corresponding site of YCpT-HSL7, yielding YCpT-GFP-HSL7, and correct orientation was confirmed by appropriate restriction endonuclease digestion.

To express from the *GAL1* promoter a version of Swe1 tagged at its N terminus with an in-frame c-Myc epitope, PCR amplification was first used to generate a derivative of the double-stranded oligonucleotide encoding the epitope (see above) containing a *Bgl*II site at its 5′ end, 5′-AGA TCT T **ATG** ATC GAA GAA CAA-3′ (*Bgl*II site underlined and start codon in bold), and a *Bam*HI site at its 3′ end, 5′-AAG AGG GAT CC-3′ (*Bam*HI site underlined). The resulting product was cleaved with *Bgl*II and *Bam*HI and ligated into the *Bam*HI site of YCpLG; a derivative with the correct orientation (as judged by restriction enzyme digestion) was designated YCpLG-Myc. Next, for other purposes, the 3′ end (codons 759 to 819) of *SWE1* was amplified by using pSWE1-14 (6) as the template and appropriate primers to introduce a *Sal*I site just upstream of the termination codon, yielding 5′-TTT ATA GTC GAC **TGA**-3′ (*Sal*I site underlined and stop codon in bold). The resulting product was ligated into the *Eco*RV site of Litmus-28, such that the end with the *Sal*I site was closest to the *Sna*BI site in the Litmus-28 polylinker, generating Litmus-28-3′-Swe1. To reconstruct the entire *SWE1* coding sequence, a 2.2-kb *Pst*I-*Acc*65I fragment, excised from pSWE1-14, and a 0.3 kb *Acc*65I-*Sna*BI fragment, excised from Litmus-28-3′-Swe1, were ligated together into *Pst*I- and *Stu*I-digested Litmus-28, yielding pMJS68. PCR with appropriate primers and pSWE1-14 as the template was used to introduce a *Bam*HI site immediately upstream of the *SWE1* initiation codon, yielding the coding sequence 5′-GGA TCC G **ATG** AGT TCT-3′ (*Bam*HI site underlined and start codon in bold). The resulting product was cleaved with *Bam*HI and *Nae*I and ligated along with a 2.3-kb *Nae*I-*Pst*I fragment excised from pMJS68 into *Bam*HI- and *Pst*I-digested YCpLG-Myc, yielding YCpLG-MycSwe1.

To express from the *GAL1* promoter a version of Hsl1 tagged at its C terminus with three tandem in-frame repeats of an epitope from the influenza virus hemagglutinin (triple-HA epitope) that is recognized by MAb 12CA5 (64, 91), a derivative of the *HSL1* coding sequence containing a *Bam*HI site immediately upstream of the termination codon was generated by PCR using pE14R1 (55) as the template and appropriate primers, yielding the sequence 5′-GCC GGA GGA TCC **TAA**-3′ (*Bam*HI site underlined and stop codon in bold). The resulting product was cleaved with *Nru*I and *Bam*HI and inserted into pDK51 (gift of D. Kellogg, University of California, Santa Cruz) that had been cleaved with *Sal*I, converted to flush ends by incubation with T4 DNA polymerase, and cleaved with *Bam*HI, yielding pMJS83. pDK51 contains the triple-HA cassette as a *Kpn*I-*Eco*RI fragment in the vector, YIplac204 (28). A derivative of *HSL1* containing a *Bgl*II site immediately upstream of the start codon and an *Nsi*I site at

the start codon was generated by PCR using pE14R1 as the template and appropriate primers, yielding 5′-AGA TCT T CGA **ATG** CAT GGT-3′ (*Bgl*II site underlined, *Nsi*I site in italics, and start codon in bold), and was cleaved with *Bgl*II and *Stu*I. The resulting fragment and a 3.5-kb *Stu*I-*Pvu*II fragment excised from pMJS83 were ligated together into YCpLG that had been cleaved with *Hin*dIII, incubated with T4 DNA polymerase, and cleaved with *Bam*HI, yielding YCpLG-HSL1$(HA)_3$. To express from the *GAL1* promoter and an internal Met codon the C-terminal 498 residues of Hsl1 tagged at its C terminus with the triple-HA epitope, a 1.6-kb *Xba*I-*Pvu*II fragment was excised from pMJS83 and inserted into YCpLG that had been cleaved with *Hin*dIII, incubated with T4 DNA polymerase, and cleaved with *Xba*I, yielding YCpLG-HSL1(1021-1518)-$(HA)_3$.

Two-hybrid screen. Strain YD116 (Table 1) harboring pAS1-HSL7 was transformed with a library of yeast cDNAs fused to the carboxyl terminus of the Gal4 transcriptional activation domain [Gal4(TAD)] driven from the *ADH1* promoter on a *LEU2*-marked 2μm DNA plasmid (gift of S. Elledge, Baylor College of Medicine, Houston, Tex.). Total number of potential transformants screened was estimated by plating appropriate dilutions of a small fraction of the transformed cells on −Trp −Leu plates to select for cells containing both *TRP1*-marked pAS1-HSL7 and a *LEU2*-marked library plasmid. Positive clones that stimulated expression of the *URA3* reporter were selected on the same medium lacking uracil and containing X-Gal, which permitted concomitant secondary screening for expression of the *lacZ* reporter. Candidate plasmids were recovered from these Ura^+ $LacZ^+$ transformants in *E. coli* (39), reintroduced into YD116 harboring pAS1-HSL7, and retested for activation of expression of the *URA3* and *lacZ* reporters. Specificity was confirmed by failure of the candidates to stimulate reporter expression in the absence of pAS1-HSL7. Candidate clones that passed all of these criteria were tested again for the ability to interact with Gal4(DBD)-Hsl7 in an independent reporter strain, Y190 (3). Partial nucleotide sequences of the inserts in the final confirmed positives were determined and identified by comparison to the *S. cerevisiae* genome database (Stanford University).

Antibodies. To prepare antigen, pGEX-Hsl7 was expressed in *E. coli* BL21(DE3)[pLysS], and the resulting GST-Hsl7 fusion protein was purified according to standard procedures. To raise polyclonal antisera, the purified GST-Hsl7 antigen was injected into adult female New Zealand White rabbits (primary inoculation, 0.5 mg; secondary boosts, 0.2 mg) and into adult female mice (primary inoculation, 100 to 200 μg; secondary boost, 100 to 200 μg) using standard methods (34). The immunoglobulin fraction was enriched from rabbit anti-Hsl7 sera by ammonium sulfate fractionation (34). Antibodies were affinity purified from mouse anti-Hsl7 sera by adsorption and elution from purified GST-Hsl7 immobilized on nitrocellulose by using minor modifications of established procedures (81, 86). Other antibodies were obtained from the following sources: mouse MAb 9E10, from S. Grell, Cancer Research Laboratory, University of California, Berkeley); mouse MAb 12CA5, (from BAbCo, Inc., or Santa Cruz Biotechnology, Inc.); and rabbit polyclonal anti-Cdc11, anti-Clb2, and anti-Swe1, from D. Kellogg.

Microscopy. Indirect immunofluorescence was performed by minor modifications of methods described in detail elsewhere (70). Briefly, exponentially growing cells were fixed with 5% formaldehyde in 0.1 M potassium phosphate (pH 6.5) containing 0.5 mM $MgCl_2$ for 30 min at room temperature and washed in 0.1 M potassium phosphate (pH 6.5). Fixed cells were resuspended in 0.2 M Tris-HCl (pH 9.0) containing 20 mM EDTA (pH 8.0), 1 M NaCl, and 80 mM β-mercaptoethanol, incubated at room temperature for 10 min, washed once with potassium phosphate-sodium citrate (pH 5.8) containing 1 M NaCl and twice with potassium phosphate-sodium citrate (pH 5.8), resuspended in 1 ml of solution A (1.2 M sorbitol, 0.1 M potassium phosphate [pH 6.5], 0.5 mM $MgCl_2$) containing 0.14 M β-mercaptoethanol, and digested with 110 μl Glusulase (NEN) and 0.6 mg of Zymolyase 100T (Seikagaku Corp., Tokyo, Japan) per ml. The digested cells were washed twice with solution A, applied to the wells of multiwell microscope slides, and permeabilized by treatment at −20°C with, successively, methanol for 6 min and acetone for 30 s. Permeabilized cells were rehydrated in phosphate-buffered saline, pH 7.3 (PBS), blocked in PBS containing 1 mg of bovine serum albumin per ml, and incubated overnight at 4°C with primary antibodies: a 1:500 dilution of affinity-purified polyclonal mouse anti-Hsl7 antibodies and a 1:500 dilution of rabbit polyclonal anti-Cdc11 antibodies (11). After incubation, cells were washed several times with PBS containing 1 mg of bovine serum albumin per ml, and incubated for 2 h in the dark with secondary antibodies: a 1:500 dilution of indocarbocyanine (Cy3)-conjugated donkey anti-mouse immunoglobulin antibody and a 1:200 dilution of fluorescein isothiocyanate (FITC)-conjugated donkey anti-rabbit antibody (both from Jackson ImmunoResearch Laboratories, Inc.). After staining, cells were washed several times with PBS and examined in an epifluorescence microscope (Zeiss) with a 100× objective lens. Images were collected by using a charge-coupled device camera (Sony) and then processed with Phase 3 imaging software (Northern Exposure, Inc.) and Photoshop (Adobe Systems, Inc.). To view cells expressing GFP-Hsl7, cultures were grown under appropriate selective conditions, and the live cells were examined directly under the fluorescence microscope equipped with an FITC band-pass filter. Images were captured and processed as described.

Coimmunoprecipitation. Protease-deficient strain BJ2168 (Table 1) carrying plasmids expressing the gene products of interest under control of the *GAL1* promoter were pregrown under appropriate selective conditions in SCRaf medium to an A_{600} of 0.6, induced by addition of galactose (2% final concentration), and incubated for 2 h. Cells were harvested, washed with PBS, and lysed by vigorous vortex mixing with glass beads in ice-cold lysis buffer (20 mM Tris-HCl [pH 7.2], 12.5 mM potassium acetate, 4 mM $MgCl_2$, 0.5 mM EDTA, 5 mM sodium bisulfite, 0.1% Tween 20, 12.5% glycerol) containing 1 mM dithiothreitol and protease inhibitors (2 μg of leupeptin per ml, 2 μg of pepstatin A per ml, 1 mM benzamidine, 2 μg of aprotinin per ml, and 1 mM phenylmethylsulfonyl fluoride). The resulting crude extracts were clarified first by centrifugation in a microcentrifuge for 10 min at 4°C and then by sedimentation at 30,000 × *g* in a table-top ultracentrifuge for 30 min at 4°C. In some experiments, two proteins of interest were coexpressed in the same cell, and then samples (1 mg of total protein) of the extracts were diluted into lysis buffer (200-μl final volume) and mixed with 20 μl of a suspension of protein A-protein G (A/G)-agarose beads (Calbiochem, Inc.). In other experiments, proteins of interest were expressed in separate cell cultures, and then samples (500 μg of total protein) of two different extracts were mixed and diluted into lysis buffer (200-μl final volume) prior to addition of the A/G-agarose beads. For preclearing, these mixtures were incubated for 1 h at 4°C on a roller drum and then subjected to centrifugation in a microcentrifuge for 5 min at 4°C. The resulting supernatant solution was transferred to a fresh tube containing another aliquot (20 μl) of A/G-agarose beads and either 1 μl of mouse ascites fluid containing anti-c-Myc MAb 9E10 or 2 μl of affinity-purified anti-HA MAb. After incubation on the roller drum for 2 h at 4°C, the bead-bound immune complexes were collected by brief centrifugation, washed three times (1 ml each) with ice-cold lysis buffer, resuspended in sample buffer for sodium dodecyl sulfate-polyacrylamide gel electrophoresis (SDS-PAGE), and solubilized by incubation in a boiling water bath for 10 min. After removal of any residual particulates by centrifugation for 10 min at room temperature, samples of the resulting supernatant fraction were resolved by SDS-PAGE, transferred to a membrane filter (Immobilon-P; Millipore) by using a semidry transfer apparatus (Bio-Rad, Inc.), analyzed by immunoblotting with appropriate primary antibodies followed by appropriate horseradish peroxidase-conjugated secondary antibodies, and visualized by using a commercial chemiluminescence detection system (Renaissance; New England Nuclear, Inc.).

Protein binding to immobilized GST fusions. Analysis of protein-protein association via interaction of soluble proteins with immobilized GST fusion proteins was performed similarly to immunoprecipitations, with the following modifications. After clarification of extracts by sedimentation in the table-top ultracentrifuge, the resulting supernatant fractions were dialyzed rapidly in a micro-concentration device (Microcon-30; Amicon, Inc.) to remove endogenous glutathione. Samples of an extract to be tested and an extract containing the GST fusion (500 μg of total protein each) were combined, diluted in lysis buffer (200-μl final volume), and mixed with a slurry of glutathione-Sepharose beads (Pharmacia). After incubation for 1 h at 4°C on a roller drum, the beads were collected and washed, and bound proteins were eluted and analyzed, all as described above for immunoprecipitations.

Assay for Swe1 modification. Cell cycle synchronization, analysis of cell cycle progression, and assessment of Swe1 hyperphosphorylation by electrophoretic mobility shift were carried out by procedures described in detail elsewhere (84), with the following modifications. To enhance sensitivity of *MAT***a** haploids to α-factor-imposed G_1 arrest, all strains used carried the *sst1-3* mutation (12) and were treated with 50 ng of α-factor per ml for 3 h at 37°C. Culture samples (1.6 ml) were taken at the indicated time points and collected by brief centrifugation, and the resulting pellets were snap frozen in liquid N_2. Frozen pellets were resuspended in 100 μl of analysis buffer (2% SDS, 50 mM Tris-HCl [pH 6.8], 100 mM dithiothreitol, 0.1% bromophenol blue, 10% glycerol) containing protease inhibitors (2 μg of leupeptin per ml, 2 μg of pepstatin A per ml, 1 mM benzamidine, 2 μg of aprotinin per ml, and 1 mM phenylsulfonyl fluoride) and phosphatase inhibitors (10 mM sodium pyrophosphate, 10 mM sodium fluoride, 5 mM sodium metavanadate, 5 mM sodium orthovanadate, 1 mM β-glycerol phosphate, and 2 μg of phosvitin per ml) and lysed by vigorous vortex mixing for 1 min with an equal volume of glass beads, followed, successively, by incubation in a boiling water bath for 1 min, vortex mixing for 1 min, and boiling for 5 min. After removal of glass beads and particulates from the solubilized material by brief centrifugation, proteins were resolved by SDS-PAGE on a 8% gel for 2 h at 200 V and analyzed by immunoblotting using either anti-Swe1 antibodies (84) or anti-Clb2 antibodies (47).

RESULTS

Hsl7 acts in a pathway that modulates tyrosine phosphorylation of Cdc28. Loss of *HSL1* or *HSL7* function causes cells to grow more slowly and to display altered morphology (55). Using either of two different deletion alleles, *hsl7-Δ10* (data not shown) and *hsl7-Δ20*, carrying different selectable markers (*URA3* and *HIS3*, respectively), we confirmed that absence of Hsl7 results in aberrant morphology in strains derived from two distinct lineages (W303 and S288C). Although the mutant cells are slightly larger than otherwise isogenic $HSL7^+$ cells (Fig. 1A), the most striking aspect of the altered morphology is

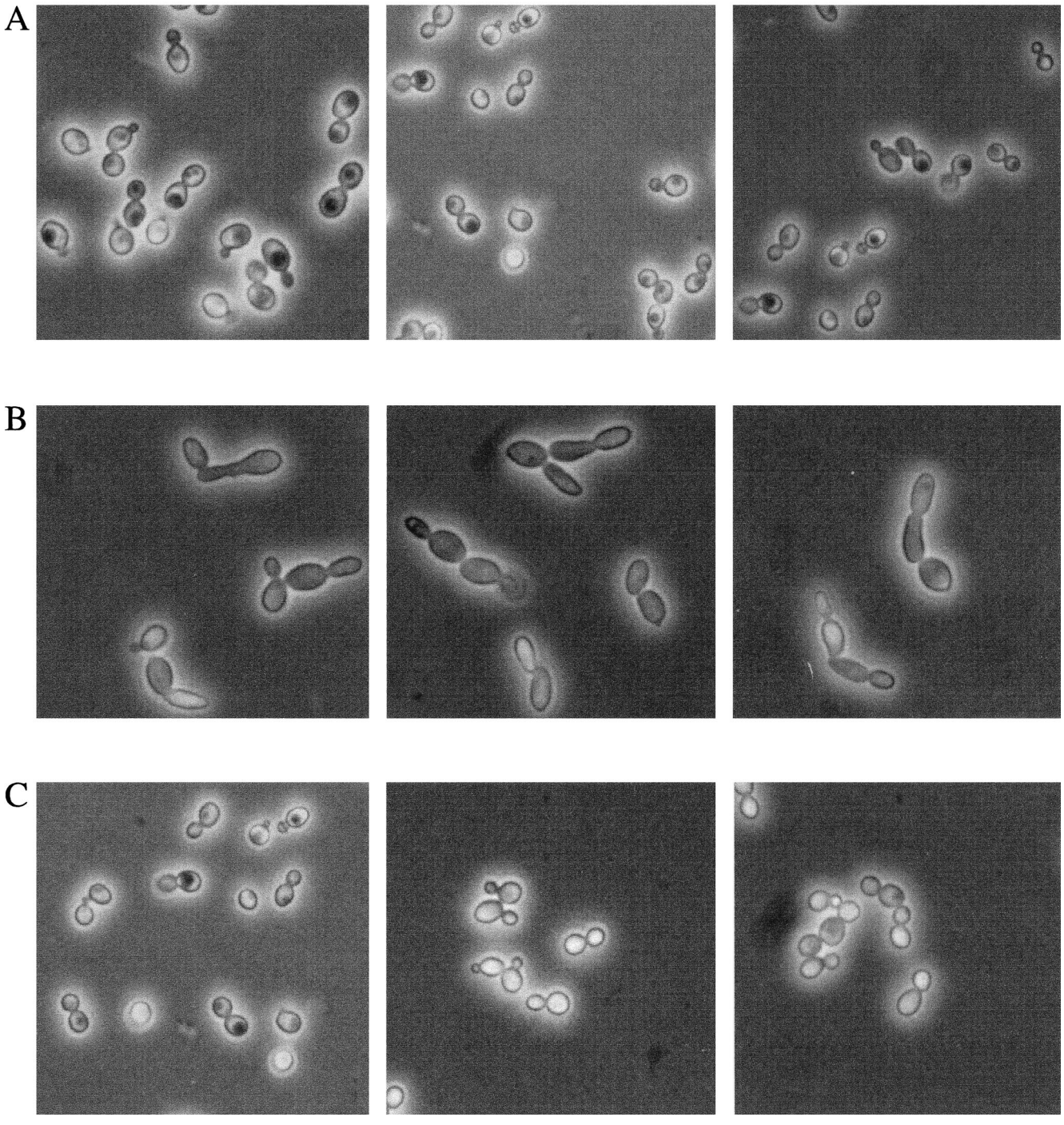

FIG. 1. Elongated bud morphology of the *hsl7*Δ mutant arises from G_2/M delay imposed by phosphorylation of Cdc28 at Tyr19. Three congenic strains, MJY112 (*HLS7*$^+$) (A), MJY102 (*hsl7*Δ) (B), and MJY124 [*hsl7*Δ *CDC28*(*Y19F*)] (C), were grown to mid-exponential phase in YPGlc at 30°C, and samples of each culture were photographed by using phase-contrast microscopy. Three independent fields are shown for each strain.

the dramatically elongated shape of the bud (Fig. 1B). Elongated buds can arise as the result of defects in genes involved directly in elaboration of the cell wall and other aspects of the actual mechanics of bud formation (reviewed in reference 14). However, elongated buds are also the hallmark of cells that have not undergone the switch from polarized to isotropic growth of the actin-based cytoskeleton (reviewed in reference 52). The transition from polarized to isotropic growth requires the function of Cdc28 complexed to B-type cyclins (Clb1 and Clb2) (51). It has already been demonstrated that the elongated bud morphology in *hsl1*Δ mutants is prevented if a *swe1*Δ mutation or a *CDC28*(*Y19F*) variant is introduced into the same cell, indicating that absence of Hsl1 causes elongated buds because Cdc28-Clb complexes are inhibited by Swe1-dependent phosphorylation at Tyr19 (55). The fact that the morphological phenotype of *hsl7*Δ cells is also suppressed by a

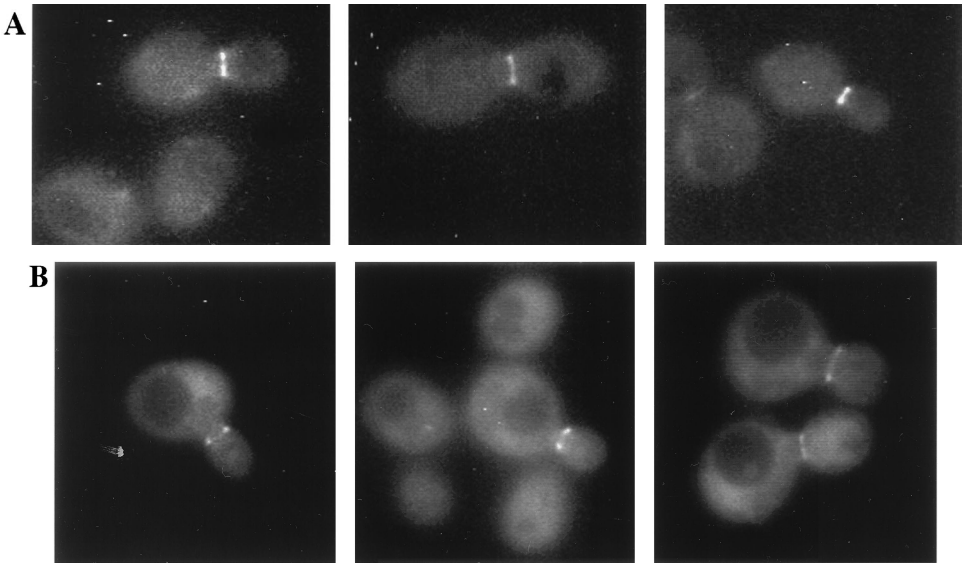
A
B

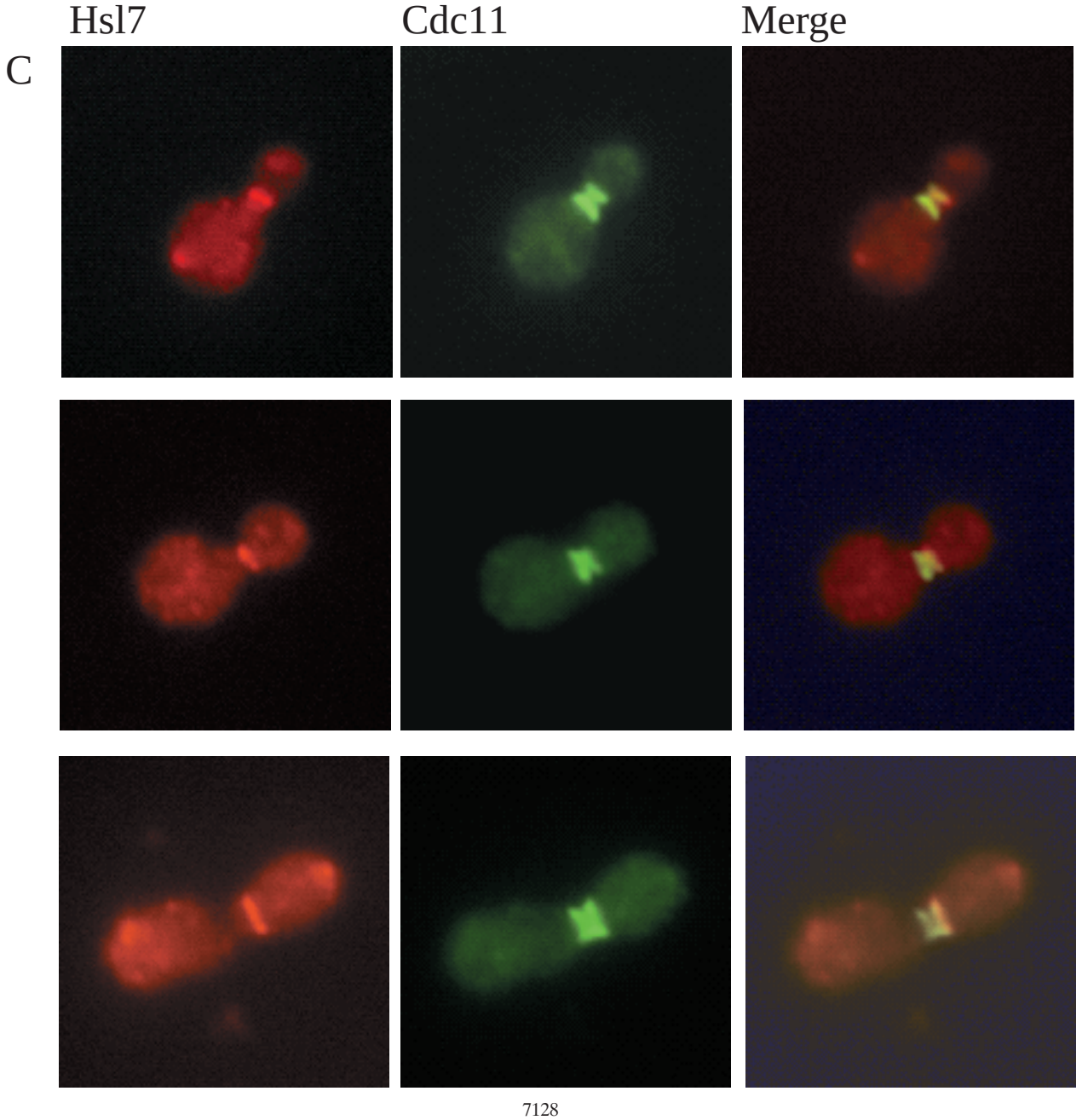
Hsl7
Cdc11
Merge
C

*swe1*Δ mutation (55), and the observation that an *hsl1*Δ *hsl7*Δ double mutant does not display a phenotype that is more severe than that of either single mutant (data not shown), suggested that Hsl7 functions in the same pathway as Hsl1. We found that the elongated bud morphology and the larger cell size of an *hsl7*Δ mutant were completely suppressed by the *CDC28*(*Y19F*) allele (Fig. 1C), confirming unequivocally that the morphological effects caused by absence of Hsl7 are mediated solely via tyrosine phosphorylation of Cdc28.

Hsl7 colocalizes with the daughter-side septin ring. It has been shown recently that Hsl1 (also known as Nik1 [87]) localizes to the neck between a mother cell and its bud and specifically decorates the bud-side septin ring (5). Likewise, two other Hsl1-related protein kinases, Gin4 (66) and Kcc4 (YCL024w) (5), also localize to the neck in a septin-dependent manner. Given the evidence that Hsl7 functions in the same pathway as Hsl1, it was important to also determine the subcellular localization of Hsl7. To address this question, we first constructed a GFP-Hsl7 fusion, which was fully functional, as judged by its ability to complement completely the morphological defect of *hsl7*Δ cells, even when expressed from the authentic *HSL7* promoter on a *CEN* plasmid (data not shown). Examination of cells expressing the GFP-Hsl7 chimera at near-normal levels from the *HSL7* promoter (Fig. 2A) or at a much higher level from the *GAL1* promoter (Fig. 2B) on *CEN* plasmids showed that the fusion protein localized as a single ring at the mother-bud junction and seemed to be more closely apposed to the bud side of the neck. This neck-specific deposition of GFP-Hsl7 was observed in cells with small, intermediate, and large buds (Fig. 2A and B); in contrast, neither a ring nor any other obvious localization of the fluorescence were detectable in unbudded cells (data not shown).

To confirm these results for native Hsl7 and to determine if the neck-specific distribution was congruent with septin localization, we raised and affinity-purified mouse polyclonal anti-Hsl7 antibodies. These antibodies are specific for Hsl7 because on immunoblots they recognized a polypeptide in extracts of wild-type cells that (i) has an apparent molecular mass, estimated from SDS-PAGE, in good agreement with that predicted for the full-length *HSL7* open reading frame (95.1 kDa); (ii) is absent in extracts from *hsl7*Δ cells; and (iii) is elevated considerably in extracts of cells expressing *HSL7* from a multicopy plasmid (data not shown). When cells were costained with the anti-Hsl7 antibodies and antibodies (11) directed against the septin, Cdc11, we observed that septin staining resolved into two separate rings (Fig. 2B), as demonstrated previously by others (54). Moreover, merging of the images showed that Hsl7 staining was coincident with, and confined to, the septin ring closest to the bud (Fig. 2C). As expected, no staining was observed with the anti-Hsl7 antibodies in *hsl7*Δ cells; however, the staining pattern for Cdc11 in the mutant cells was not detectably different from that seen in wild-type cells (data not shown). Thus, like Hsl1, Hsl7 localizes only to the daughter-side septin ring and only in budded cells, but is not required for septin ring formation. Hence, the subcellular distribution of both Hsl1 and Hsl7 is highly specific in both a spatial and a temporal sense. Moreover, the localization of

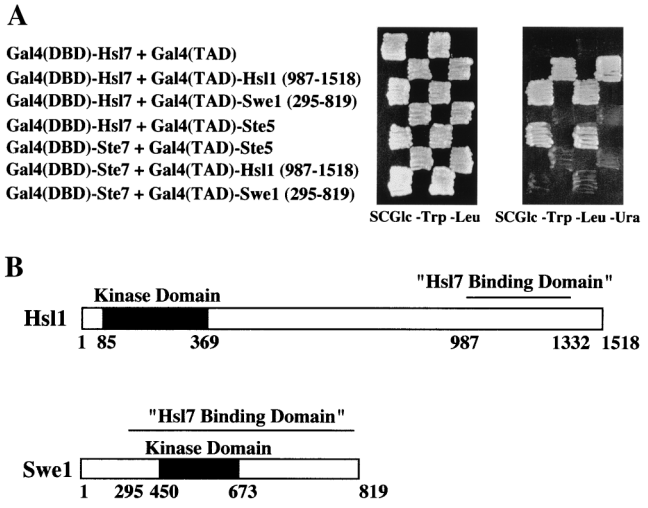

FIG. 3. A two-hybrid screen identifies both Hsl1 and Swe1 as Hsl7-interacting proteins. (A) A reporter strain (YD116) in which *URA3* expression is *GAL1* promoter dependent was cotransformed with a plasmid expressing a Gal4(DBD)-Hsl7 chimera and plasmids expressing either Gal4(TAD) alone (top row), Gal4(TAD)-Hsl1(987-1518) (second row), Gal4(TAD)-Swe1(295-819) (third row), or, as an additional negative control, Gal4(TAD)-Ste5 (fourth row). The same strain was cotransformed with a plasmid expressing Gal4(DBD)-Ste7 and plasmids expressing, as a positive control, either Gal4(TAD)-Ste5 (fifth row), Gal4(TAD)-Hsl1(987-1518) (sixth row), or Gal4(TAD)-Swe1(295-819) (last row) to demonstrate specificity. (B) Schematic diagrams of the primary structure of the Hsl1 and Swe1 protein kinases. Catalytic domain (solid box), noncatalytic regions (open boxes), and the minimal Hsl7-binding domain (overlined) in each protein, as delineated by the smallest common segment shared by the corresponding clones isolated in the two-hybrid screen, and their relative sequence positions (numbers below) are indicated.

Hsl7 revealed by these studies, and the fact that Hsl7 is not required for septin ring formation, suggested that it could participate directly in monitoring formation of the daughter septin ring (or another component that interacts with that ring) and thus could be intimately involved in the septin assembly checkpoint.

Identification of proteins that interact with Hsl7. Although genetic evidence suggests that Hsl7 acts in the same pathway as Hsl1 to negatively regulate Swe1 (55), it was unclear whether Hsl7 acts directly on Hsl1 or on Swe1, or indirectly via interaction with a septin or another protein (such as the Mih1 phosphatase), to alleviate the Swe1-dependent phosphorylation of Cdc28 at Tyr19. To gain further insight about the role of Hsl7 in these processes in an unbiased manner, we used the two-hybrid method to screen a total yeast cDNA library for gene products capable of interacting with Hsl7. For this purpose, we constructed a plasmid that constitutively expressed a Gal4(DBD)-Hsl7 fusion. Stable expression of the fusion was confirmed by immunoblotting with anti-Hsl7 antibodies (data not shown). When the Gal4(DBD)-Hsl7 fusion was expressed in an *hsl7*Δ mutant, normal morphology was restored to the vast majority of (but not all) cells (data not shown), suggesting that the chimera is able to supply *HLS7* function, but may do

FIG. 2. Both a GFP-Hsl7 chimera and native Hsl7 localize to the daughter-side septin ring. Strain MJY112 cells transformed with *CEN* plasmids expressing GFP-Hsl7 from either the authentic *HSL7* promoter (A) or the *GAL1* promoter (B) were grown to mid-exponential phase at 30°C in SCGlc-Trp or SCRaf-Leu (followed by induction with 2% galactose for 2 h), respectively, and samples of each culture were viewed directly in a fluorescence microscope, as described in Materials and Methods. Strain MJY112 was grown to mid-exponential phase in YPGlc at 30°C, fixed, permeabilized, costained with affinity-purified mouse anti-Hsl7 antibodies (detected with a Cy3-labeled secondary antibody) and with purified rabbit antibodies directed against the septin, Cdc11 (detected with a FITC-labeled secondary antibody), and viewed in the fluorescence microscope, as described in Materials and Methods (C). Three different individual cells are shown, and the images were merged by using appropriate computer software, as described in Materials and Methods.

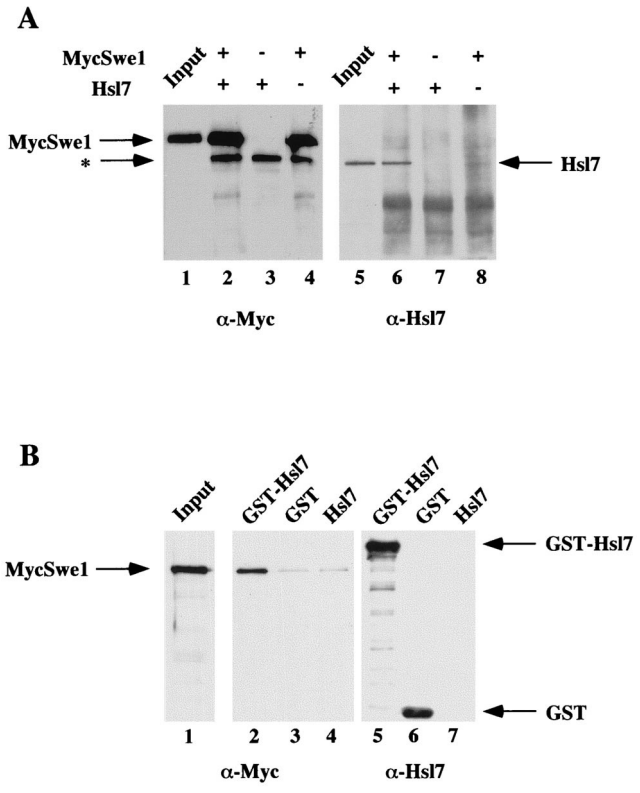

FIG. 4. Hsl7 physically associates with Swe1 in cell extracts. (A) Extracts of protease-deficient cells expressing either MycSwe1 or Hsl7 were prepared. Equivalent amounts of total protein from these extracts were incubated either alone or together, as indicated, and then subjected to immunoprecipitation using anti-c-Myc MAb 9E10. The resulting immunoprecipitates were resolved by SDS-PAGE and analyzed by immunoblotting either with MAb 9E10 to detect MycSwe1 (left) or with purified rabbit polyclonal anti-Hsl7 antibodies (right). Samples representing ~1% of the extracts added to each incubation (Input) were examined on the same gels. The asterisk denotes a species present in mouse ascites fluid that adsorbs to the A/G-agarose beads used for immunoprecipitation and nonspecifically cross-reacts with the horseradish peroxidase-linked goat anti-mouse immunoglobulin used for detection of the primary antibody (MAb 9E10). (B) Extracts of protease-deficient cells expressing GST, GST-Hsl, or Hsl7 were prepared. Equivalent amounts of total protein from these extracts were mixed with identical amounts of an extract containing MycSwe1 and then incubated with glutathione-agarose beads. After washing the beads, bound proteins were resolved by SDS-PAGE and analyzed by immunoblotting with mouse anti-Hsl7 antibodies (which were raised against an GST-Hsl7 fusion) to demonstrate specific binding of GST and GST-Hsl7 to the beads (right) and with MAb 9E10 to detect the presence of MycSwe1 (middle). A sample representing ~1% of the MycSwe1-containing extract added to each incubation (Input) was examined on the same gel (left).

so less efficiently than native Hsl7 because some fraction of the hybrid protein is presumably directed to the nucleus via the Gal4(DBD). To identify interacting proteins, cells expressing Gal4(DBD)-Hsl7 were transformed with the library of cDNAs fused to the Gal4(TAD) in a reporter strain (YD116) in which restoration of *GAL* promoter-dependent transcriptional transactivation drives both *URA3* and *lacZ* expression. From approximately 7×10^6 total transformants screened, 200 Ura^+ $LacZ^+$ colonies were obtained initially. Library plasmids were rescued from half of these original positives. Of these 100 candidates, 30 were able to reproducibly stimulate reporter gene expression in a Gal4(DBD)-Hsl7-dependent manner in both YD116 and an independent tester strain (Y190 [Table 1]). The identity of the gene products in these inserts was deduced by nucleotide sequence analysis and querying of the *Saccharomyces* genome database by computer, using standard search algorithms.

Of the 30 plasmids characterized, the majority (i.e., 19) contained in common the Gal4(TAD) fused to an overlapping internal segment of *ADE13*, which encodes adenylosuccinate lyase, an enzyme that catalyzes reactions essential for synthesis of IMP and for conversion of IMP to AMP (43). We assume that their interaction with Gal4(DBD)-Hsl7 is an artifact because this region of Ade13 is presumably buried in the interior of the native enzyme. Likewise, three of the plasmids encoded "junk" inserts that were clearly generated by ligation of sequences derived from at least two different loci. Revealing, however, of the remaining eight plasmids, three encoded fusions of the C-terminal third of Hsl1 to the Gal4(TAD) and two encoded fusions of most of Swe1 to the Gal4(TAD) (Fig. 3A). None of the three Hsl1 isolates contained its kinase domain, and the smallest overlapping segment shared by the three inserts delineated the Hsl7-binding domain of Hsl1 (residues 987 to 1332) (Fig. 3B). In contrast, the Swe1 isolates contained its kinase domain and lacked only the first 294 residues of the protein (Fig. 3B). None of the Gal4(TAD)-Hsl1 or Gal4(TAD)-Swe1 fusions was able to activate reporter expression in the absence of Gal4(DBD)-Hsl7 (Fig. 3A). In addition, specificity of these interactions was further demonstrated by the findings that Gal4(DBD)-Hsl7 did not interact with an irrelevant Gal4(TAD) fusion, Gal4(TAD)-Ste5 (40), and that none of the Gal4(TAD)-Hsl1 or Gal4(TAD)-Swe1 fusions could interact with an irrelevant Gal4(DBD) fusion, Gal4(DBD)-Ste7 (40). In light of the previous genetic evidence, these findings strongly suggest that Hsl7 acts by physically associating with both Hsl1 and Swe1 and assisting in some fashion with the Hsl1-dependent phosphorylation of Swe1.

The remaining three Gal4(TAD) clones isolated as interacting with Gal4(DBD)Hsl7 contained fusions to a previously uncharacterized open reading frame (YNL094w), which we have found encodes a protein that localizes to actin patches, as will be described in detail elsewhere (78a).

Hsl7 associates with Hsl1 and Swe1 in cell extracts. To confirm the results of the two-hybrid screen by an independent biochemical method and to determine whether native Hsl7 can interact with full-length Hsl1 and full-length Swe1, we examined whether these proteins bind tightly enough to each other to be coimmunoprecipitated. First, in the process of investigating the interaction between Hsl7 and Swe1, we found that we were unable to cooverexpress *HSL7* and *SWE1* efficiently in the same cell. Consequently, we prepared separate cell extracts, one from a protease-deficient strain (BJ2168) overexpressing *HSL7* and another from the same strain overexpressing a fully functional derivative of *SWE1* tagged at its N terminus with a c-Myc epitope (MycSwe1), after each was induced briefly (2 h) from the *GAL1* promoter on a *CEN* plasmid. Equivalent amounts of these extracts, either alone or mixed with each other, were subjected to immunoprecipitation with the anti-c-Myc MAb 9E10. The resulting immunoprecipitates were resolved by SDS-PAGE and transferred to a filter, and the proteins present were analyzed by immunoblotting with appropriate antibodies. As expected, MycSwe1 was efficiently immunoprecipitated by the anti-c-Myc MAb in either the presence or absence of the Hsl7-containing extract (Fig. 4A, left). Conversely, Hsl7 was not nonspecifically absorbed by the anti-c-Myc MAb. Strikingly, however, Hsl7 was efficiently coimmunoprecipitated in the sample that contained both MycSwe1 and Hsl7 (Fig. 4A, right), demonstrating the presence of MycSwe1-Hsl7 complexes. To confirm the tight association of Hsl7 and Swe1 in the reverse manner, we also examined the ability of GST-Hsl7 to bind MycSwe1 in solution. In this ex-

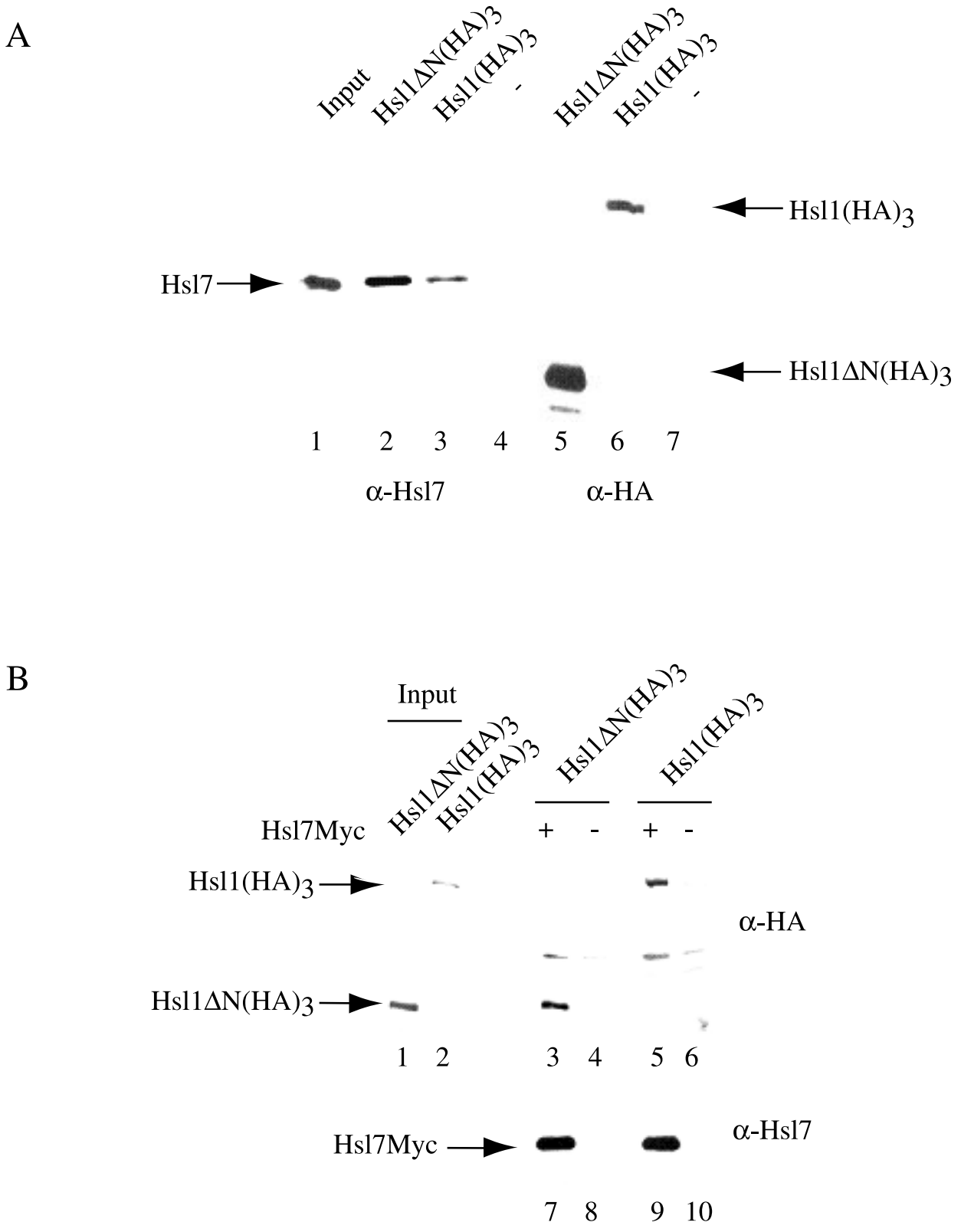

FIG. 5. Hsl7 physically associates with Hsl1 in cell extracts. (A) Extracts of protease-deficient cells expressing Hsl7 alone (−) or Hsl7 coexpressed with either full-length Hsl1 tagged with a triple-HA epitope [Hsl1(HA)$_3$] or a C-terminal fragment, Hsl1(1021-1518), tagged with the same epitope [Hsl1ΔN(HA)$_3$], as indicated, were prepared. Equivalent amounts of protein from these extracts were subjected to immunoprecipitation with mouse anti-HA MAb 12CA5. The immunoprecipitates were resolved by SDS-PAGE and analyzed by immunoblotting with MAb 12CA5 to demonstrate specific recovery of the tagged proteins (right) and with rabbit anti-Hsl7 antibodies to detect the presence of Hsl7 (left). As a marker, a sample representing ~1% of the Hsl7-containing extract (Input) was analyzed on the same gel. (B) Extracts of protease-deficient cells expressing either Hsl1-HA$_3$ or Hsl1ΔN-HA$_3$, as indicated, coexpressed with either Myc-tagged Hsl7(+) or an empty vector (−), were prepared. Equivalent amounts of protein from these extracts were subjected to immunoprecipitation with anti-Myc MAb 9E10. The immunoprecipitates were resolved by SDS-PAGE and analyzed by immunoblotting with mouse anti-Hsl7 antibodies to confirm expression of Hsl7 (bottom) and with the anti-HA MAb to detect the presence of the HA-tagged Hsl1 derivatives (top). Samples representing ~1% of the Hsl1-HA$_3$- and Hsl1ΔN-HA$_3$-containing extracts (Input) were also analyzed as markers.

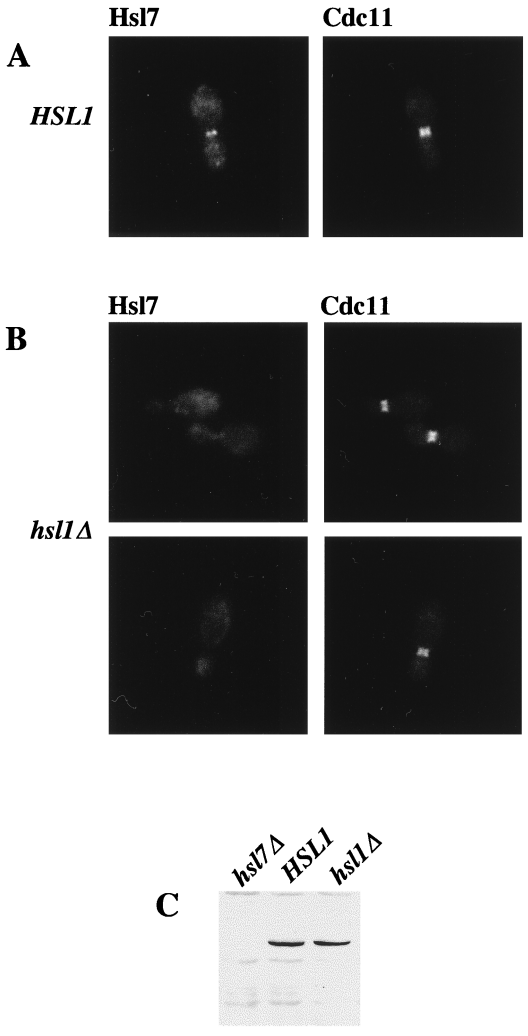

FIG. 6. Localization of Hsl7 at the bud neck requires Hsl1. An *HSL1*$^+$ strain (MJY112; A) and an otherwise isogenic *hsl1*Δ derivative (MJY141; B) were grown to mid-exponential phase in YPGlc at 30°C, then costained for Hsl7 and for the septin, Cdc11, and viewed by indirect immunofluorescence, as described in the legend to Fig. 2. To confirm that stable expression of Hsl7 does not require Hsl1, samples (40 μg of total protein) of cell extracts from the same strains and from an otherwise isogenic *hsl7*Δ strain (MJY102) were prepared, resolved by SDS-PAGE, and analyzed by immunoblotting with mouse anti-Hsl7 antibodies (C).

periment, extract containing MycSwe1 was mixed with extracts from BJ2168 that expressed either GST alone, GST-Hsl7, or underivatized Hsl7. After incubation, protein complexes were captured on glutathione-agarose beads. Bound proteins were resolved by SDS-PAGE, transferred to a filter, and analyzed by immunoblotting with appropriate antibodies. We found that GST alone and GST-Hsl7 were efficiently retained by the beads, but not free Hsl7, as expected (Fig. 4B, right panel). Reassuringly, MycSwe1 was bound specifically only to the beads that were exposed to GST-Hsl7 and not to the beads exposed to GST alone or to underivatized Hsl7 (Fig. 4B, left). Thus, full-length Hsl7 and full-length Swe1 are able to physically associate.

To investigate interaction between Hsl7 and Hsl1, extracts were prepared from strain BJ2168 cooverexpressing both *HSL7* and derivatives of *HSL1* tagged at their C termini with a triple-HA epitope, after each was induced briefly (2 h) from the *GAL1* promoter on a *CEN* plasmid. These extracts were subjected to immunoprecipitation with anti-HA MAb 12CA5, and the immune complexes were analyzed by SDS-PAGE, transfer to a filter, and immunoblotting with appropriate antibodies. Both full-length Hsl1 and a fragment representing the C-terminal third of Hsl1 (residues 1021 to 1518) were efficiently expressed and immunoprecipitated (Fig. 5A, right), as expected. Hsl7 was not nonspecifically absorbed by the anti-HA MAb in extracts lacking an HA-tagged protein. In contrast, we reproducibly observed that a modest amount of Hsl7 coimmunoprecipitated with full-length Hsl1-HA_3 (Fig. 5A, left). Most strikingly, however, and in agreement with the results of the two-hybrid screen, the segment of Hsl1 corresponding to its C-terminal 498 residues, tagged with HA_3, appeared to coimmunoprecipitate Hsl7 much more efficiently than full-length Hsl1. To confirm association of Hsl7 and Hsl1 in the reverse manner, we cooverexpressed in BJ2168 either an empty vector or Hsl7 tagged at its C terminus with a c-Myc epitope with either Hsl1-HA_3 or Hsl1(1021-1518)-HA_3, subjected the resulting extracts to immunoprecipitation with anti-c-Myc MAb, and analyzed the immune complexes by SDS-PAGE and immunoblotting. As expected, Hsl7-Myc was efficiently expressed and immunoprecipitated by the anti-Myc MAb (Fig. 5B, right). In separate experiments, we showed that underivatized Hsl7 is not nonspecifically absorbed by the anti-Myc MAb (data not shown). Once again, we found that full-length Hsl1-HA_3 was inefficiently coimmunoprecipitated with Hsl7-Myc (but always reproducibly above the background), whereas Hsl1(1021-11518)-HA_3 was coimmunoprecipitated very efficiently (Fig. 5B, left). Thus, although full-length Hsl7 can physically associate with full-length Hsl1, this interaction seems to be enhanced markedly by removal of the amino-terminal portion of Hsl1, which contains its catalytic domain.

Localization of Hsl7 is dependent on Hsl1. The findings that (i) Hsl7 directly interacts with Hsl1, as judged both by the two-hybrid method in vivo and by coimmunoprecipitation in vitro, and (ii) both proteins localize to a septin ring raised the issue of the order in which the septin-Hsl1-Hsl7 complexes are assembled. It has already been demonstrated that Hsl1 localization is dependent on proper septin assembly (5). Likewise, we found that GFP-Hsl7 was completely delocalized when a temperature-sensitive septin *cdc10* mutant was shifted to the restrictive temperature (data not shown). Thus, both proteins are targeted to the bud neck in a septin-dependent manner. In this regard, it has been shown by others that Hsl1 coimmunoprecipitates with the septin, Cdc3 (5). We have confirmed this observation and, moreover, found that full-length Hsl1 coimmunoprecipitates with other septins, specifically, Cdc10 and Cdc11 (data not shown). In contrast, the HA_3-tagged C-terminal fragment of Hsl1 (residues 1021 to 1518), despite its ability to interact efficiently with Hsl7, does not target to the bud neck, as judged by indirect immunofluorescence with anti-HA antibodies (data not shown), suggesting that the septin-binding domain of Hsl1 lies elsewhere in the molecule. Although interaction of Hsl1 with septins can be demonstrated by coimmunoprecipitation, we have been unable under any condition tested to coimmunoprecipitate Hsl7 with any of three septins (Cdc3, Cdc10, and Cdc11) (data not shown). Taken together, these results suggested that the normal order of events involves septin assembly, followed by docking of Hsl1 and then recruitment of Hsl7. Indeed, in agreement with this scenario, it has been reported that Hsl1 localizes to the bud neck in an *hsl7*Δ mutant (unpublished results cited in reference 5).

To explore the converse relationship, we used indirect immunofluorescence to examine whether localization of Hsl7 to the septin ring is dependent on Hsl1. In normal (*HSL1*$^+$)

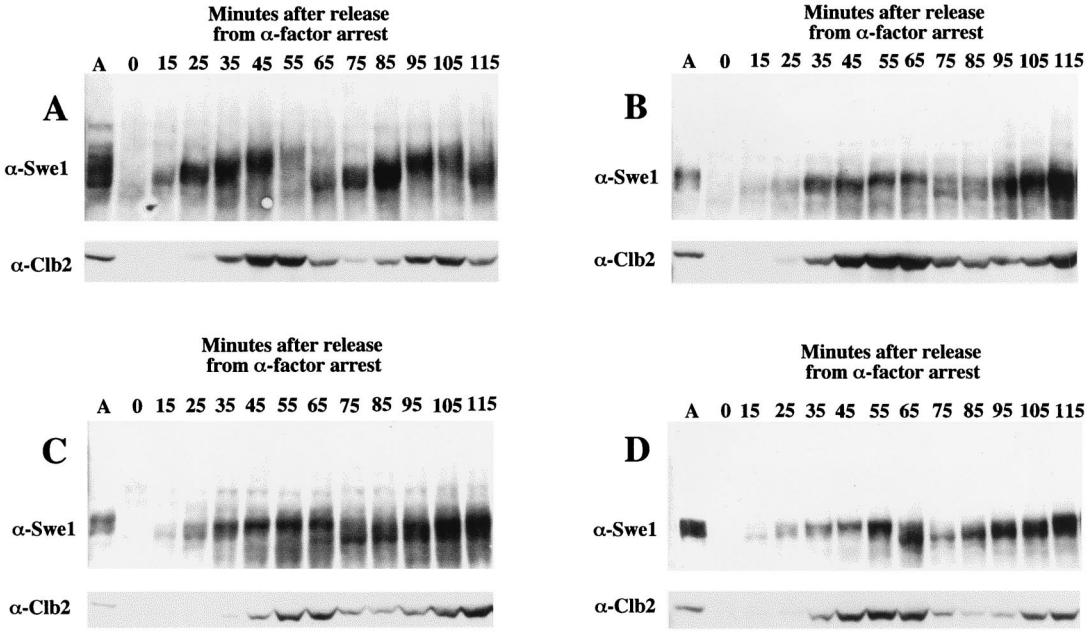

FIG. 7. Modification of Swe1 requires Hsl1 and Hsl7. A *MAT***a** *HSL1*$^+$ *HSL7*$^+$ strain (MJY155; A) and its otherwise isogenic *hsl1*Δ (MJY157; B), *hsl7*Δ (MJY156; C), and *hsl1*Δ *hsl7*Δ (MJY158; D) derivatives were grown to mid-exponential phase in YPGlc at 30°C, and samples of these asynchronous cultures (lane A in each panel) were withdrawn prior to treatment with pheromone, resolved by SDS-PAGE, and analyzed by immunoblotting with anti-Swe1 and anti-Clb2 antibodies. Portions of the same cultures were then synchronized by arrest with α-factor, as described in Materials and Methods. After release from the pheromone-imposed block, samples were taken at the time intervals indicated and the status of Swe1 and Clb2 was analyzed in the same fashion.

budded cells, Hsl7 colocalizes at the bud neck with the septin rings (Fig. 6A), as we have shown above. In marked contrast, in an otherwise isogenic *hsl1*Δ mutant, no localization of Hsl7 at the bud neck is detectable, both in cells with grossly elongated buds (data not shown) and in cells with buds of near-normal morphology (Fig. 6B). One potential explanation for this result might be that Hsl7 is unstable and rampantly degraded in *hsl1*Δ cells; however, this trivial possibility was ruled out by immunoblot analysis, which revealed that *hsl1*Δ mutants and *HSL1*$^+$ cells contain equivalent amounts of Hsl7 polypeptide (Fig. 6C). Costaining of the same cells for the septin, Cdc11, revealed that the septin rings are present and properly assembled at the bud neck in the *hsl1*Δ mutant (compare Fig. 6A and B). Thus, mislocalization of Hsl7 is most likely the direct result of the absence of Hsl1, rather than due to a general defect in septin ring organization. Consistent with these results, we also found that GFP-Hsl7 chimera is not localized to the bud neck in an *hsl1*Δ mutant (data not shown). Collectively, these observations support the conclusion that septin assembly is normal in the absence of Hsl1 or Hsl7 and that Hsl1 is indeed responsible for recruiting Hsl7 to the bud neck, thereby providing additional evidence that Hsl1 interacts with Hsl7 in vivo.

Hsl1 and Hsl7 are required for efficient phosphorylation and degradation of Swe1. During the G_2-M transition, Swe1 becomes hyperphosphorylated and then degraded by ubiquitin-mediated proteolysis (45, 80). Ubiquitinylation of Swe1 is mediated by a so-called SCF complex that depends on a linker protein (Skp1), a specific ubiquitin-conjugating enzyme (Cdc34), and a targeting subunit (Met30) that contains an F-box motif (45). As observed for the destruction of other substrates by related SCF complexes, phosphorylation of the target to be destroyed is a prelude to its recognition by the cognate SCF (reviewed in references 50 and 69). Hyperphosphorylated forms of Swe1 can be detected readily as slower-migrating species by SDS-PAGE (80, 84). The Hsl1 homolog in *S. pombe*, Nim1/Cdr1, has been shown to phosphorylate directly and inhibit the activity of the *S. pombe* Swe1 homolog, Wee1 (15). The fact that Hsl7 interacts by the two-hybrid screen and by coimmunoprecipitation with both Swe1 and Hsl1 suggested that its function may be to deliver and/or present Swe1 to Hsl1 to permit its efficient Hsl1-dependent phosphorylation. To test this hypothesis, we examined the state of modification of Swe1 in *hsl1*Δ and *hsl7*Δ single mutants, in an *hsl1*Δ *hsl7*Δ double mutant, and in the otherwise isogenic *HSL1*$^+$ *HSL7*$^+$ parental strain. We analyzed the distribution of Swe1-related species both in asynchronous cultures at steady state and in cultures that were synchronized by mating pheromone-imposed G_1 arrest and then released from that block (see Materials and Methods).

In normal cells in asynchronous culture, immunoblots of Swe1 reproducibly showed multiple (at least six) species of distinct electrophoretic mobility (Fig. 7A). By contrast, in *hsl1*Δ, *hsl7*Δ, and *hsl1*Δ *hsl7*Δ cells, we observed only a prominent doublet that migrated with the species of most rapid electrophoretic mobility (Fig. 7B to D). In normal cells synchronized by arrest with mating pheromone, released from the block, and followed through approximately two cell cycles, the electrophoretic mobility of Swe1 increased progressively and then the bulk of the protein disappeared, concomitant with progression through G_2/M as marked by the accumulation and destruction of the B-type cyclin, Clb2 (Fig. 7A). In the *hsl1*Δ, *hsl7*Δ, and *hsl1*Δ *hsl7*Δ cells, however, the kinetics of both the modification and disappearance of Swe1 were markedly retarded. Consistent with the genetic findings suggesting that Hsl7 and Hsl1 function in the same pathway (55), the reduction in the Swe1 electrophoretic mobility shift was no more severe in the *hsl1*Δ *hsl7*Δ double mutant (Fig. 7D) than in the corresponding single mutants (Fig. 7B and C). These results indicate that Hsl1 is responsible for most, but not all, of the

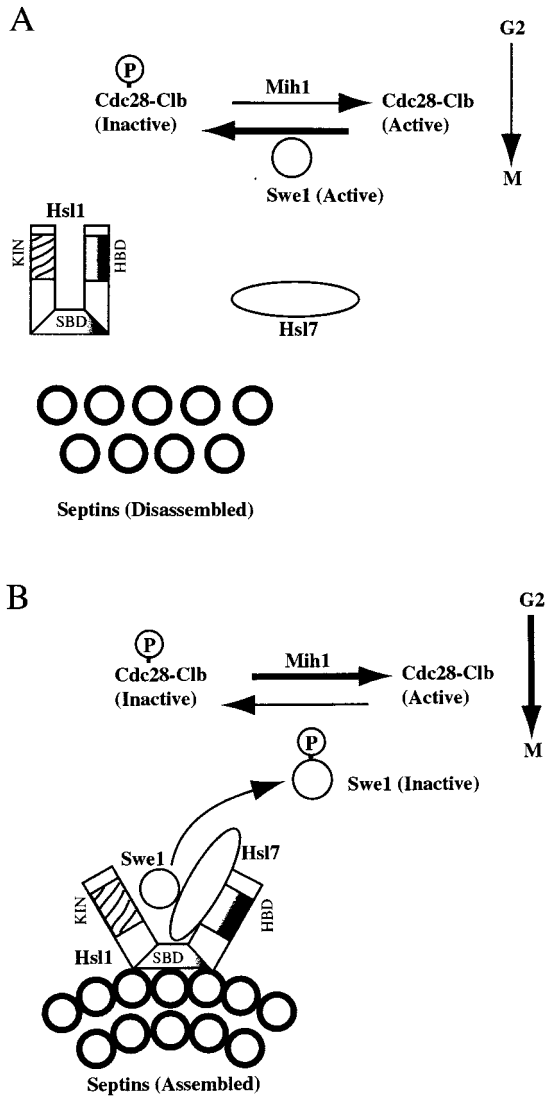

FIG. 8. Model for the role of Hsl1 and Hsl7 in linking septin ring assembly to activation of Cdc28-Clb complexes. See Discussion for details. The catalytic domain (KIN), Hsl7-binding domain (HDB), and postulated septin-binding domain (SBD) of Hsl1 are indicated.

modification of Swe1 that causes its electrophoretic mobility shift. Given that two other Hsl1 homologs, Gin4 and Kcc4, are present in the *S. cerevisiae* genome, these other protein kinases may also contribute to the phosphorylation of Swe1, albeit to a lesser extent than Hsl1. In addition, these findings confirm that in the absence of Hsl7, Hsl1 cannot function to modify Swe1. Finally, in the *hsl1*Δ, *hsl7*Δ, and *hsl1*Δ *hsl7*Δ cells, Clb2 appears with essentially normal kinetics, suggesting that the absence of the most slowly migrating forms of Swe1 is not due to generally faulty cell cycle progression or a failure of cells to advance into G_2/M.

DISCUSSION

This study addressed how Hsl7 functions, at the mechanistic level, as a negative regulator of the Swe1 protein kinase. We found that Hsl7 is localized specifically to the bud neck, congruent with the septin ring closest to the daughter cell. We also found, using both genetic and biochemical methods, that Hsl7 physically associates with the Hsl1 protein kinase, another known negative regulator of Swe1 (55), as well as with Swe1 itself. In agreement with these findings, we showed that targeting of Hsl7 to the bud neck requires Hsl1. Moreover, we demonstrated that Hsl7 is required for the Hsl1- and cell cycle-dependent modification and destruction of Swe1. We feel that our results, and the previous observations of others, are best explained by the following model (Fig. 8).

A mechanism for coupling septin ring assembly to inactivation of Swe1. Both Hsl1 (170 kDa) and Hsl7 (95 kDa) are large molecules. In the absence of either Hsl1 or Hsl7, cells are viable and the septin rings seem to form normally at the bud neck, whereas defective septin function is lethal to the cell, suggesting that both Hsl1 and Hsl7 act downstream of septin assembly. As shown recently by Barral et al. (5), the Hsl1 protein kinase localizes to the bud-side septin ring, but in the absence of functional septins, Hsl1 is not present at the bud neck. These workers also demonstrated, by coimmunoprecipitation, that Hsl1 physically associates with at least one septin, Cdc3. Hence, it seems likely that septin assembly recruits Hsl1 to the ring. Moreover, these investigators found that functional septins are required to activate the catalytic activity of Hsl1, suggesting that interaction of this enzyme with the septins causes a conformational change that exposes its N-terminal kinase domain. Correspondingly, it seems that Hsl7 associates only weakly with full-length Hsl1 but binds strongly to the C-terminal 498 residues of Hsl1, as might be expected if the proposed septin-induced conformational change in Hsl1 also exposes its C terminus, permitting the docking of Hsl7.

Additional observations are consistent with this order of events. First, we showed that localization of Hsl7 to the bud-side septin ring requires the presence of Hsl1, whereas it has been reported that docking of Hsl1 to the septin ring does not require Hsl7 (5). Second, unlike Hsl1, we found that Hsl7 was unable to coimmunoprecipitate any of three different septins tested. Third, we have found that overproduction of the C-terminal 498 residues of Hsl1 displaces GFP-Hsl7 from the bud neck (78b). Finally, this C-terminal fragment of Hsl1 does not itself localize to the bud neck, suggesting that other regions of Hsl1 are required for its targeting to the septin ring.

Given that Hsl7 and Swe1 interact via the two-hybrid method in the nucleus (where Hsl1 is presumably absent) and given that Hsl7 and Swe1 coimmunoprecipitate efficiently when overproduced (and are presumably present in large excess over the normal cellular level of Hsl1), we favor the idea that the exposed C terminus of Hsl1 directly recruits a preformed Hsl7-Swe1 complex, thereby permitting the kinase domain of Hsl1 to efficiently phosphorylate Swe1. Thus, Hsl7 acts as an adapter to direct Swe1 specifically to Hsl1. We cannot rule out, however, the possibility that binding of Hsl7 to the C terminus of Hsl1 further enhances the affinity of Hsl7 (or Hsl1) for Swe1 (and/or that binding of Hsl7 to the C terminus of Hsl1 changes the substrate specificity or further stimulates the catalytic activity of Hsl1). Moreover, whether Hsl1, Hsl7, and Swe1 can bind simultaneously to each other to form ternary complexes has not yet been examined experimentally; however, bacterially expressed GST-Hsl1(ΔN) and GST-Swe1 (but not empty beads or GST alone) can bind radiolabeled Hsl7 prepared by in vitro translation in reticulocyte lysates, supporting the conclusion that the interactions between these proteins are direct (78c). The effect of Hsl7 binding alone on the ability of Swe1 to phosphorylate Cdc28-Clb complexes has not yet been explored; however, since the phenotype of *hsl1*Δ *hsl7*Δ mutants is no more severe than that of either single mutant, it seems unlikely that Hsl7 acts as an independent inhibitor of Swe1. In any event, it seems almost certain that Hsl1, a Nim1

homolog, is responsible for phosphorylation of Swe1, a Wee1 homolog, because it has been shown that heterologously expressed and purified *S. pombe* Nim1 can phosphorylate and inhibit the activity of *S. pombe* Wee1 (15, 68, 92). In agreement with this supposition, we found that modification of Swe1 was severely compromised in either an *hsl7*Δ or an *hsl1*Δ mutant, as judged by a greatly reduced electrophoretic mobility shift.

Because Swe1 is responsible for inhibition of Cdc28-Clb complexes by phosphorylation at Tyr19, which causes a G_2/M delay (6), the Hsl1- and Hsl7-dependent inactivation of Swe1 permits reactivation of Clb-bound Cdc28 via the action of the Mih1 phosphatase. Recent results indicate that this switch is made essentially irreversible because phosphorylation of Swe1 leads to its ubiquitinylation and proteasome-dependent proteolysis (45, 80). There is some evidence that Cdc28 activity may be required for the degradation of Swe1 (80); hence, Hsl1-dependent phosphorylation of Swe1 may be necessary, but not sufficient, to set this process in motion. Moreover, it seemed at least feasible that Clb-bound Cdc28 is the protein kinase directly responsible for Swe1 phosphorylation (rather than Hsl1 per se) because in the absence of Hsl1 (and/or Hsl7), Swe1 is hyperactive, leading to inhibition of Cdc28 via its phosphorylation at Tyr19. We examined the effect of deleting Hsl1 (and Hsl7) on Swe1 phosphorylation in a cell in which the only form of Cdc28 present is the Y19F mutant, which confers resistance to Swe1-mediated inhibition, and found that the absence of Hsl1 (and Hsl7) still largely abrogates Swe1 phosphorylation (78c). Hence, it appears that Hsl1, and not Cdc28, is the kinase responsible for much of the observed modification of Swe1. Consistent with a role for Hsl7 in delivering Swe1 to Hsl1 and with a role for Hsl1-dependent phosphorylation as a primary event in triggering Swe1 destruction, the rate of Swe1 disappearance seemed somewhat reduced in either an *hsl7*Δ or an *hsl1*Δ mutant. The existence of two additional Hsl1-related protein kinases, Gin4 and Kcc4, which are localized to the bud neck and appear to act in a manner at least partially redundant with Hsl1 (5), may explain why the G_2/M delay observed in an *hsl1*Δ or *hsl7*Δ mutant is not a permanent arrest and why modification of Swe1 is largely, but not completely, eliminated in an *hsl1*Δ or *hsl7*Δ mutant.

Thus, collectively, our results suggest a reasonable mechanism for how septin assembly stimulates Hsl1 and how Hsl7 cooperates with Hsl1 to negatively regulate Swe1. Inactivation of Swe1, in turn, relieves the inhibition of Cdc28-Clb complexes, thereby permitting passage through G_2/M. Thus, Hsl7 serves a key function in a pathway that links proper formation of the septin rings to cell cycle progression.

Hsl1 and Hsl7 constitute a septin assembly checkpoint pathway. A physiological role for modulation of Cdc28 activity by phosphorylation at Tyr19 was obscure until recently because of the previous demonstration that a Y19F mutation in Cdc28 had no obvious effect on the delay in entering mitosis elicited in response to DNA damage or unreplicated DNA (2, 82). However, Swe1-dependent inhibitory phosphorylation at Tyr19 occurs during the G_2 delay evoked by inhibiting bud formation (79), and this regulation of Cdc28-Clb complexes appears to be the basis of a morphogenesis checkpoint that monitors the state of assembly of the actin cytoskeleton (53, 56). Likewise, Swe1-dependent phosphorylation of Cdc28-Clb appears to be responsible for a G_2 delay caused by defective septin ring assembly (5). Thus, Swe1 is the target of at least two pathways that monitor different aspects of cell morphology.

Given the roles of Hsl1 and Hsl7 in down-regulating Swe1 in normal mitosis, it seems clear how these same proteins also concomitantly provide a built-in checkpoint mechanism that impedes passage through G_2/M in the absence of correct septin ring assembly. If septin assembly is prevented, Hsl1 cannot dock on the septin ring and an Hsl1-Hsl7 complex cannot form. Hence, Swe1 is not delivered to Hsl1 and not inactivated by phosphorylation. Since the level of active Swe1 remains high, Cdc28-Clb complexes will be phosphorylated at Tyr19, imposing a G_2 delay. Moreover, since Cdc28 activity may be required, in addition to phosphorylation by Hsl1, to initiate the ubiquitin-dependent proteolysis of Swe1 (51, 80), Swe1-mediated inhibition of Cdc28-Clb complexes further protects Swe1 from inactivation and sustains the G_2 delay. This idling presumably would provide an opportunity for proper septin assembly. However, once septin ring formation occurs, the Hsl1-Hsl7 complex forms, inactivates Swe1, alleviating the inhibition of Cdc28-Clb complexes, thus allowing the cell to progress into mitosis.

Hsl7 may regulate Swe1 only in the bud. Septin ring-dependent and Hsl1- and Hsl7-mediated inactivation of Swe1 also promotes another event that requires active Cdc28-Clb complex. Prior to mitosis, the bud grows in a polarized fashion at its tip; however, when the cell enters mitosis, bud growth switches from this anisotropic mode to an isotropic pattern in which the bud expands over its entire surface, thus forming a rounded structure (reviewed in reference 20). Experimental evidence indicates that this morphological transition requires active Cdc28-Clb complexes (51). Our findings suggest that septin ring assembly, and the ensuing Hsl1- and Hsl7-mediated inactivation of Swe1, must precede initiation of the switch from polarized to isotropic growth. Consistent with this conclusion, cells lacking Hsl1 or Hsl7 display marked elongated buds, as shown here and by others (55). This phenotype is also observed in septin mutants, in agreement with the suggestion that septin ring formation is a prelude to isotropic growth (11).

In terms of a septin assembly checkpoint per se, it is unclear why (and how) Hsl7 and Hsl1 are asymmetrically distributed to the septin ring that faces the daughter cell. It is possible that assembly of the bud-side septin ring requires a properly assembled mother-side ring; thus, by associating with the bud-side ring, Hsl1 and Hsl7, in effect, assess formation of the entire twin-ring structure. Alternatively, however, localization of Hsl1 and Hsl7 to the daughter-side ring may indicate that these proteins have a more significant role in ensuring efficiency of the switch from polarized to isotropic bud growth. By being stationed at the opening of the narrow isthmus between the mother cell and the bud, Hsl1 and Hsl7 may act as gatekeepers to specifically prevent active Swe1 from entering the bud. As a consequence, Cdc28-Clb activity may first become activated locally in the bud. Presumably Cdc28-Clb complexes regulate proteins that are involved in a variety of events, only a subset of which are involved in the switch from polarized to isotropic growth. Nonetheless, these particular substrates of Cdc28-Clb are likely to be located in the bud.

Conservation of this mechanism. In addition to Swe1 in *S. cerevisiae*, all other eukaryotes examined to date, including *Drosophila melanogaster* (10), frogs (60), and humans (67), possess a homolog of *S. pombe* Wee1 protein kinase. Likewise, homologs of budding yeast Hsl7 are found in fission yeast (30), flies (56a), *Caenorhabditis elegans* (55), and humans (49). Similarly, like *S. cerevisiae* Hsl1, Gin4, and Kcc4, there are multiple apparent Nim1 homologs in *S. pombe* (7, 46, 75) and in the worm (13) and fly (9a) genomes. Although these proteins have been conserved during evolution, available evidence suggests that their functions may have diverged somewhat in different organisms. In budding yeast, loss of Swe1 does not detectably perturb cell cycle kinetics under normal growth conditions (6), whereas absence of Wee1 in fission yeast results in premature entry into mitosis, leading to smaller average cell size (74).

Correspondingly, Cdc25, the phosphatase that removes the inhibitory phosphate from Tyr15 in Cdc2, is essential for the viability of fission yeast (73), but its budding yeast counterpart, Mih1, is dispensable (72). Phosphorylation of Tyr15 in Cdc2 is involved in both the DNA replication and DNA damage checkpoints in fission yeast, whereas phosphorylation of Tyr19 in Cdc28 has no apparent role in these events (reviewed in reference 71). Nevertheless, it is now clear that phosphorylation of Tyr19 in Cdc28 is pivotal both in the morphogenesis checkpoint that monitors assembly of actin-based structures (56) and, as we have shown here, in the checkpoint that gauges assembly of the septin-based rings (5). Our results demonstrate unequivocally, in agreement with previous genetic findings (55), that Hsl1 and Hsl7 function to inactivate Swe1 in budding yeast and, hence, act as mitotic activators. However, it has been reported recently that the Hsl7 homolog in fission yeast, Skb1, acts as a mitotic inhibitor (29), although neither its relationship to Nim1 and Wee1 nor its localization has been investigated directly. Given that septins are found ubiquitously and are localized at the site of cell division in all eukaryotes (16, 54), we suspect that the homologs of Hsl1, Hsl7, and Swe1 will perform, as in *S. cerevisiae*, a function in linking proper septin assembly to passage through mitosis to ensure optimal timing of cell cycle progression.

ACKNOWLEDGMENTS

We thank Namrita Dhillon, Tim Durfee, Bob Booher, Michael Grunstein, and Steve Elledge for strains and plasmids, Stevan Marcus and Mike Snyder for the communication of results prior to publication, and members of the Drubin/Barnes laboratory for assistance with fluorescence microscopy. We especially thank Doug Kellogg for antibodies, plasmids, and the communication of unpublished results.

This work was supported by NIH predoctoral traineeship GM07232 and a William V. Power Graduate Fellowship (to M.J.S.) and by NIH research grant GM21841 and facilities provided by the Berkeley campus Cancer Research Laboratory (to J.T.).

REFERENCES

1. **Alani, E., L. Cao, and N. Kleckner.** 1987. A method for gene disruption that allows repeated use of URA3 selection in the construction of multiply disrupted yeast strains. Genetics **116:**541–545.
2. **Amon, A., U. Surana, I. Muroff, and K. Nasmyth.** 1992. Regulation of p34^{cdc28} tyrosine phosphorylation is not required for entry into mitosis in *S. cerevisiae*. Nature **355:**368–371.
3. **Bai, C., and S. J. Elledge.** 1996. Gene identification using the yeast two-hybrid system. Methods Enzymol. **273:**331–347.
4. **Bardwell, L., J. G. Cook, J. X. Zhu-Shimoni, D. Voora, and J. Thorner.** 1998. Differential regulation of transcription: repression by unactivated mitogen-activated protein kinase Kss1 requires the Dig1 and Dig2 proteins. Proc. Natl. Acad. Sci. USA **95:**15400–15405.
5. **Barral, Y., M. Parra, S. Bidlingmaier, and M. Snyder.** 1999. Nim1-related kinases coordinate cell-cycle progression with the organization of the peripheral cytoskeleton in yeast. Genes Dev. **13:**176–187.
6. **Booher, R. N., R. J. Deshaies, and M. W. Kirschner.** 1993. Properties of the *Saccharomyces cerevisiae* wee1 and its differential regulation of p34^{cdc28} in response to G_1 and G_2 cyclins. EMBO J. **12:**3417–3426.
7. **Breeding, C. S., J. Hudson, M. K. Balasubramanian, S. M. Hemmingsen, P. G. Young, and K. L. Gould.** 1998. The cdr2(+) gene encodes a regulator of G2/M progression and cytokinesis in Schizosaccharomyces pombe. Mol. Biol. Cell **9:**3399–3415.
8. **Byers, B., and L. Goetsch.** 1976. Loss of the filamentous ring in cytokinesis-defective mutants of budding yeast. J. Cell Biol. **70:**35 (Abstract.)
9. **Byers, B., and L. Goetsch.** 1976. A highly ordered ring of membrane-associated filaments in budding yeast. J. Cell Biol. **69:**717–721.
9a. **Campbell, S., (University of Alberta, Edmonton, Alberta, Canada).** Personal communication.
10. **Campbell, S. D., F. Sprenger, B. A. Edgar, and P. H. O'Farrell.** 1995. Drosophila Wee1 kinase rescues fission yeast from mitotic catastrophe and phosphorylates Drosophila Cdc2 in vitro. Mol. Biol. Cell **6:**1333–1347.
11. **Carroll, C. W., R. Altman, D. Schieltz, J. R. Yates III, and D. Kellogg.** 1998. The septins are required for the mitosis-specific activation of the Gin4 kinase. J. Cell Biol. **143:**709–717.
12. **Chan, R. K., and C. A. Otte.** 1982. Isolation and genetic analysis of *Saccharomyces cerevisiae* mutants supersensitive to G_1 arrest by a factor and alpha factor pheromones. Mol. Cell. Biol. **2:**11–20.
13. **Chervitz, S. A., L. Aravind, G. Sherlock, C. A. Ball, E. V. Koonin, S. S. Dwight, M. A. Harris, K. Dolinski, S. Mohr, T. Smith, et al.** 1998. Comparison of the complete protein sets of worm and yeast: orthology and divergence. Science **282:**2022–2028.
14. **Cid, V. J., A. Duran, F. del Rey, M. P. Snyder, C. Nombela, and M. Sanchez.** 1995. Molecular basis of cell integrity and morphogenesis in *Saccharomyces cerevisiae*. Microbiol. Rev. **59:**345–386.
15. **Coleman, T. R., Z. Tang, and W. G. Dunphy.** 1993. Negative regulation of the wee1 protein kinase by direct action of the nim1/cdr1 mitotic inducer. Cell **72:**919–929.
16. **Cooper, J. A., and D. P. Kiehart.** 1996. Septins may form a ubiquitous family of cytoskeletal filaments. J. Cell Biol. **134:**1345–1348.
17. **Cvrckova, F., C. De Virgilio, E. Manser, J. R. Pringle, and K. Nasmyth.** 1995. Ste20-like protein kinases are required for normal localization of cell growth and for cytokinesis in budding yeast. Genes Dev. **9:**1817–1830.
18. **Davis, T. N., and J. Thorner.** 1989. Vertebrate and yeast calmodulin, despite significant sequence divergence, are functionally interchangeable. Proc. Natl. Acad. Sci. USA **86:**7909–7913.
19. **DeMarini, D. J., A. E. M. Adams, H. Fares, C. DeVirgilio, G. Valle, J. S. Chuang, and J. R. Pringle.** 1997. A septin-based hierarchy of proteins required for localized deposition of chitin in the *Saccharomyces cerevisiae* cell wall. J. Cell Biol. **139:**75–93.
20. **Drubin, D. G., and W. J. Nelson.** 1996. Origins of cell polarity. Cell **84:**335–344.
21. **Durfee, T., K. Becherer, P. L. Chen, S. H. Yeh, Y. Yang, A. E. Kilburn, W. H. Lee, and S. J. Elledge.** 1993. The retinoblastoma protein associates with the protein phosphatase type 1 catalytic subunit. Genes Dev. **7:**555–569.
22. **Evan, G. I., G. K. Lewis, G. Ramsay, and J. M. Bishop.** 1985. Isolation of monoclonal antibodies specific for human *c-myc* proto-oncogene product. Mol. Cell. Biol. **5:**3610–3616.
23. **Evans, P. D., S. N. Cook, P. D. Riggs, and C. J. Noren.** 1995. LITMUS: multipurpose cloning vectors with a novel system for bidirectional in vitro transcription. BioTechniques **19:**130–135.
24. **Feinberg, A. P., and B. Vogelstein.** 1984. Addendum: a technique for radiolabeling DNA restriction endonuclease fragments to high specific activity. Anal. Biochem. **137:**266–267.
25. **Feldmann, H., M. Aigle, G. Aljinovic, B. Andre, M. C. Baclet, C. Barthe, A. Baur, A. M. Becam, N. Biteau, E. Boles, et al.** 1994. Complete DNA sequence of yeast chromosome II. EMBO J. **13:**5795–5809.
25a. **Field, C. M., O. al-Awar, J. Rosenblatt, M. L. Wong, B. Alberts, and T. J. Mitchison.** 1996. A purified Drosophila septin complex forms filaments and exhibits GTPase activity. J. Cell Biol. **133:**605–616.
26. **Fitch, I., C. Dahmann, U. Surana, A. Amon, K. Nasmyth, L. Goetsch, B. Byers, and B. Futcher.** 1992. Characterization of four B-type cyclin genes of the budding yeast Saccharomyces cerevisiae. Mol. Biol. Cell **3:**805–818.
27. **Frazier, J. A., M. L. Wong, M. S. Longtine, J. R. Pringle, M. Mann, T. J. Mitchison, and C. Field.** 1998. Polymerization of purified yeast septins: evidence that organized filament arrays may not be required for septin function. J. Cell Biol. **143:**737–749.
28. **Gietz, R. D., and A. Sugnino.** 1988. New yeast-*Escherichia coli* shuttle vectors constructed with *in vitro* mutagenized yeast genes lacking six-base pair restriction sites. Gene **74:**527–534.
29. **Gilbreth, M., P. Yang, G. Bartholomeusz, R. A. Pimental, S. Kansra, R. Gadiraju, and S. Marcus.** 1998. Negative regulation of mitosis in fission yeast by the shk1 interacting protein skb1 and its human homolog, Skb1Hs. Proc. Natl. Acad. Sci. USA **95:**14781–14786.
30. **Gilbreth, M., P. Yang, D. Wang, J. Frost, A. Polverino, M. H. Cobb, and S. Marcus.** 1996. The highly conserved *skb1* gene encodes a protein that interacts with Shk1, a fission yeast Ste20/PAK homolog. Proc. Natl. Acad. Sci. USA **93:**13802–13807.
31. **Gould, K. L., and P. Nurse.** 1989. Tyrosine phosphorylation of the fission yeast cdc2+ protein kinase regulates entry into mitosis. Nature **342:**39–45.
32. **Hanahan, D.** 1983. Studies on transformation of *Escherichia coli* with plasmids. J. Mol. Biol. **166:**557–580.
33. **Hardwick, K. G.** 1998. The spindle checkpoint. Trends Genet. **14:**1–4.
34. **Harlow, E., and D. Lane.** 1988. Antibodies: a laboratory manual. Cold Spring Harbor Laboratory, Cold Spring Harbor, N.Y.
35. **Hartwell, L.** 1971. Genetic control of the cell division cycle in yeast. IV. Genes controlling bud emergence and cytokinesis. Exp. Cell Res. **69:**265–276.
36. **Hartwell, L., T. Weinert, L. Kadyk, and B. Garvik.** 1994. Cell cycle checkpoints, genomic integrity, and cancer. Cold Spring Harbor Symp. Quant. Biol. **59:**259–263.
37. **Hartwell, L. H., J. Culotti, J. R. Pringle, and B. J. Reid.** 1974. Genetic control of the cell division cycle in yeast. Science **183:**46–51.
38. **Hartwell, L. H., and T. A. Weinert.** 1989. Checkpoints: controls that ensure the order of cell cycle events. Science **246:**629–634.
39. **Hoffman, C. S., and F. Winston.** 1987. A ten-minute DNA preparation from yeast efficiently releases autonomous plasmids for transformation of Escherichia coli. Gene **57:**267–272.

40. **Inouye, C., N. Dhillon, T. Durfee, P. C. Zambryski, and J. Thorner.** 1997. Mutational analysis of STE5 in the yeast Saccharomyces cerevisiae: application of a differential interaction trap assay for examining protein-protein interactions. Genetics **147:**479–492.
41. **Johnston, M., and R. W. Davis.** 1984. Sequences that regulate the divergent *GAL1-GAL10* promoter in Saccharomyces cerevisiae. Mol. Cell. Biol. **4:**1440–1448.
42. **Jones, E. W.** 1991. Tackling the protease problem in yeast. Methods Enzymol. **194:**428–453.
43. **Jones, E. W., and G. R. Fink.** 1982. Regulation of amino acid and nucleotide biosynthesis in yeast, p. 181–299. *In* J. N. Strathern, E. W. Jones, and J. R. Broach (ed.), The molecular biology of the yeast Saccharomyces: metabolism and gene expression. Cold Spring Harbor Laboratory Press, Cold Spring Harbor, N.Y.
44. **Jones, J. S., and L. Prakash.** 1990. Yeast *Saccharomyces cerevisiae* selectable markers in pUC18 polylinkers. Yeast **6:**363–366.
45. **Kaiser, P., R. A. L. Sia, E. G. S. Bardes, D. J. Lew, and S. I. Reed.** 1998. Cdc34 and the F-box protein Met30 are required for degradation of the Cdk-inhibitory kinase Swe1. Genes Dev. **12:**2587–2597.
46. **Kanoh, J., and P. Russell.** 1998. The protein kinase Cdr2, related to Nim1/Cdr1 mitotic inducer, regulates the onset of mitosis in fission yeast. Mol. Biol. Cell **9:**3321–3334.
47. **Kellogg, D. R., and A. W. Murray.** 1995. Nap1 acts with Clb2 to perform mitotic functions and suppress polar bud growth in budding yeast. J. Cell Biol. **130:**675–685.
48. **Kinoshita, M., S. Kumar, A. Mizoguchi, C. Ide, A. Kinoshita, T. Haraguchi, Y. Hiraoka, and M. Noda.** 1997. Nedd5, a mammalian septin, is a novel cytoskeletal component interacting with actin-based structures. Genes Dev. **11:**1535–1547.
49. **Krapivinsky, G., W. Pu, K. Wickman, L. Krapivinsky, and D. E. Clapham.** 1998. pICIn binds to a mammalian homolog of a yeast protein involved in regulation of cell morphology. J. Biol. Chem. **273:**10811–10814.
50. **Krek, W.** 1998. Proteolysis and the G1-S transition: the SCF connection. Curr. Opin. Genet. Dev. **8:**36–42.
51. **Lew, D. J., and S. I. Reed.** 1993. Morphogenesis in the yeast cell cycle: regulation by Cdc28 and the cyclins. J. Cell Biol. **120:**1305–1320.
52. **Lew, D. J., and S. I. Reed.** 1995. Cell cycle control of morphogenesis in budding yeast. Curr. Opin. Genet. Dev. **5:**17–23.
53. **Lew, D. J., and S. I. Reed.** 1995. A cell cycle checkpoint monitors morphogenesis in budding yeast. J. Cell Biol. **129:**739–749.
54. **Longtine, M. S., D. J. DeMarini, M. L. Valencik, O. S. Al-War, H. Fares, C. De Virgilio, and J. R. Pringle.** 1996. The septins: roles in cytokinesis and other processes. Curr. Opin. Cell. Biol. **8:**106–119.

54a. **Longtine, M. S., H. Fares, and J. R. Pringle.** 1998. Role of the yeast Gin4p protein kinase in septin assembly and the relationship between septin assembly and septin function. J. Cell Biol. **143:**719–736.

55. **Ma, X.-J., Q. Lu, and M. Grunstein.** 1996. A search for proteins that interact genetically with histone H3 and H4 amino termini uncovers novel regulators of the Swe1 kinase in *Saccharomyces cerevisiae*. Genes Dev. **10:**1327–1340.
56. **McMillan, J. N., R. A. L. Sia, and D. J. Lew.** 1998. A morphogenesis checkpoint monitors the actin cytoskeleton in yeast. J. Cell Biol. **142:**1487–1499.

56a. **Mechler, B. M. (German Cancer Research Center, Heidelberg, Germany).** Personal communication.

57. **Mendenhall, M. D., and A. E. Hodge.** 1998. Regulation of Cdc28 cyclin-dependent protein kinase activity during the cell cycle of the yeast Saccharomyces cerevisiae. Microbiol. Mol. Biol. Rev. **62:**1191–1243.
58. **Mitchell, D. A., T. K. Marshall, and R. J. Deschenes.** 1993. Vectors for the inducible overexpression of glutathione S-transferase fusion proteins in yeast. Yeast **9:**715–722.
59. **Morgan, D. O.** 1997. Cyclin-dependent kinases: engines, clocks, and microprocessors. Annu. Rev. Cell Dev. Biol. **13:**261–291.
60. **Mueller, P. R., T. R. Coleman, and W. G. Dunphy.** 1995. Cell cycle regulation of a Xenopus Wee1-like kinase. Mol. Biol. Cell **6:**119–134.
61. **Muhua, L., N. R. Adames, M. D. Murphy, C. R. Shields, and J. A. Cooper.** 1998. A cytokinesis checkpoint requiring the yeast homologue of an APC-binding protein. Nature **393:**487–491.
62. **Nasmyth, K.** 1993. Control of the yeast cell cycle by the Cdc28 protein kinase. Curr. Opin. Cell Biol. **5:**166–179.
63. **Neufeld, T. P., and G. M. Rubin.** 1994. The *Drosophila peanut* gene is required for cytokinesis and encodes a protein similar to yeast putative bud neck filament proteins. Cell **77:**371–379.
64. **Niman, H. L., R. A. Houghten, L. E. Walker, R. A. Reisfeld, I. A. Wilson, J. M. Hogle, and R. A. Lerner.** 1983. Generation of protein-reactive antibodies by short peptides is an event of high frequency: implications for the structural basis of immune recognition. Proc. Natl. Acad. Sci. USA **80:**4949–4953.
65. **Nurse, P.** 1997. Checkpoint pathways come of age. Cell **91:**865–867.
66. **Okuzaki, D., S. Tanaka, H. Kanazawa, and H. Nojima.** 1997. Gin4 of S. cerevisiae is a bud neck protein that interacts with the Cdc28 complex. Genes Cells **2:**753–770.
67. **Parker, L. L., P. J. Sylvestre, M. J. Byrnes III, F. Liu, and H. Piwnica-Worms.** 1995. Identification of a 95-kDa WEE1-like tyrosine kinase in HeLa cells. Proc. Natl. Acad. Sci. USA **92:**9638–9642.
68. **Parker, L. L., S. A. Walter, P. G. Young, and H. Piwnica-Worms.** 1993. Phosphorylation and inactivation of the mitotic inhibitor Wee1 by the *nim1*/*cdr1* kinase. Nature **363:**736–738.
69. **Patton, E. E., A. R. Willems, and M. Tyers.** 1998. Combinatorial control in ubiquitin-dependent proteolysis: don't Skp the F-Box hypothesis. Curr. Opin. Genet. Dev. **14:**236–243.
70. **Pringle, J. R., A. E. M. Adams, D. G. Drubin, and B. Haarer.** 1991. Immunofluorescence methods for yeast. Methods Enzymol. **194:**565–602.
71. **Rhind, N., and P. Russell.** 1998. Mitotic DNA damage and replication checkpoints in yeast. Curr. Opin. Cell Biol. **10:**749–758.
72. **Russell, P., S. Moreno, and S. I. Reed.** 1989. Conservation of mitotic controls in fission and budding yeast. Cell **57:**295–303.
73. **Russell, P., and P. Nurse.** 1986. cdc25^{+} functions as an inducer in the mitotic control of fission yeast. Cell **45:**569–576.
74. **Russell, P., and P. Nurse.** 1987. Negative regulation of mitosis by *wee1*$^{+}$, a gene encoding a protein kinase homolog. Cell **49:**559–567.
75. **Russell, P., and P. Nurse.** 1987. The mitotic inducer nim1+ functions in a regulatory network of protein kinase homologs controlling the initiation of mitosis. Cell **49:**569–576.
76. **Sambrook, J., E. F. Fritsch, and T. Maniatis.** 1989. Molecular cloning: a laboratory manual, 2nd ed. Cold Spring Harbor Laboratory Press, Cold Spring Harbor, N.Y.
77. **Sanger, F., S. Nicklen, and A. R. Coulson.** 1977. DNA sequencing with chain-terminating inhibitors. Proc. Natl. Acad. Sci. USA **74:**5463–5467.
78. **Sherman, F., G. R. Fink, and J. B. Hicks.** 1986. Laboratory course manual for methods in yeast genetics. Cold Spring Harbor Laboratory, Cold Spring Harbor, N.Y.

78a. **Shulewitz, M. J., L. Tseng, and J. Thorner.** Unpublished data.
78b. **Shulewitz, M. J., and L. Tseng.** Unpublished data.
78c. **Shulewitz, M. J.** Unpublished data.

79. **Sia, R. A., H. A. Herald, and D. J. Lew.** 1996. Cdc28 tyrosine phosphorylation and the morphogenesis checkpoint in budding yeast. Mol. Biol. Cell **7:**1657–1666.
80. **Sia, R. A. L., E. S. G. Bardes, and D. J. Lew.** 1998. Control of Swe1p degradation by the morphogenetic checkpoint. EMBO J. **17:**6678–6688.
81. **Smith, D. E., and P. A. Fisher.** 1984. Identification, developmental regulation, and response to heat shock of two antigenically related forms of a major nuclear envelope protein in Drosophila embryos: application of an improved method for affinity purification of antibodies using polypeptides immobilized on nitrocellulose blots. J. Cell Biol. **99:**20–28.
82. **Sorger, P. K., and A. W. Murray.** 1992. S-phase feedback control in budding yeast independent of tyrosine phosphorylation of p34^{cdc28}. Nature **355:**365–368.
83. **Southern, E. M.** 1975. Detection of specific sequences among DNA fragments separated by gel electrophoresis. J. Mol. Biol. **98:**503–517.
84. **Sreenivasan, A., and D. Kellogg.** The roles of the Elm1 and Swe1 kinases in the control of mitotic events in budding yeast. Submitted for publication.
85. **Straight, A. F.** 1997. Cell cycle: checkpoint proteins and kinetochores. Curr. Biol. **7:**R613–R616.
86. **Talian, J. C., J. B. Olmsted, and R. D. Goldman.** 1983. A rapid procedure for preparing fluorescein-labeled specific antibodies from whole antiserum: its use in analyzing cytoskeletal architecture. J. Cell Biol. **97:**1277–1282.
87. **Tanaka, S., and H. Nojima.** 1996. Nik1: a Nim1-like protein kinase of S. cerevisiae interacts with the Cdc28 complex and regulates cell cycle progression. Genes Cells **1:**905–921.
88. **Thomas, B. J., and R. Rothstein.** 1989. Elevated recombination rates in transcriptionally active DNA. Cell **56:**619–630.
89. **Tourret, J., and F. McKeon.** 1996. Tyrosine kinases wee1 and mik1 as effectors of DNA replication checkpoint control. Prog. Cell Cycle Res. **2:**91–97.
90. **Weinert, T.** 1998. DNA damage and checkpoint pathways: molecular anatomy and interactions with repair. Cell **94:**555–558.
91. **Wilson, I. A., H. L. Niman, R. A. Houghten, A. R. Cherenson, M. L. Connolly, and R. A. Lerner.** 1984. The structure of an antigenic determinant in a protein. Cell **37:**767–778.
92. **Wu, L., and P. Russell.** 1993. Nim1 kinase promotes mitosis by inactivating Wee1 tyrosine kinase. Nature **363:**738–741.
93. **Yanisch-Perron, C., J. Vieira, and J. Messing.** 1985. Improved M13 phage cloning vectors and hos strains: nucleotide sequences of the M13mp18 and pUC19 vectors. Gene **33:**103–119.